

THE FAR FIELD ANALYSIS OF PARALLEL  
PLATE LUNEBERG LENSES FOR VARIOUS FEEDS

Robert Boyd Birchfield

Library  
Naval Postgraduate School  
Monterey, California 93940

# NAVAL POSTGRADUATE SCHOOL

## Monterey, California



# THESIS

THE FAR FIELD ANALYSIS  
OF  
PARALLEL PLATE LUNEBERG LENSES FOR VARIOUS FEEDS

by

Robert Boyd Birchfield

Thesis Advisor:

R. W. Adler

September 1973

T 156430

*Approved for public release; distribution unlimited.*



The Far Field Analysis  
of  
Parallel Plate Luneberg Lenses for Various Feeds

by

Robert Boyd Birchfield  
Lieutenant, United States Navy  
B.S., Purdue University, 1966  
M.S., Naval Postgraduate School, 1973

Submitted in partial fulfillment of the  
requirements for the degree of

ELECTRICAL ENGINEER

from the  
NAVAL POSTGRADUATE SCHOOL  
September 1973



## ABSTRACT

This thesis developed expressions for the aperture fields and integral equations for the far field radiation characteristics of the Parallel Plate Luneberg Lens Microwave Antenna operating in the TEM or  $TE_{10}$  modes. These expressions were programmed on a digital computer to predict the far field radiation patterns for several feed systems. Experimentation produced far field radiation patterns that were very close to the theoretical patterns for the  $TE_{10}$  mode lens and substantially different for the TEM mode lens.



# TABLE OF CONTENTS

|      |   |    |
|------|---|----|
| I.   | INTRODUCTION - - - - -                                  | 7  |
| II.  | THEORETICAL ANALYSIS - - - - -                          | 10 |
|      | A. RAY PATHS - - - - -                                  | 11 |
|      | B. APERTURE FIELD - - - - -                             | 13 |
|      | C. ELECTROMAGNETIC FIELD CALCULATIONS - - - - -         | 18 |
| III. | EXPERIMENTAL VERIFICATION - - - - -                     | 22 |
|      | A. DISCUSSION - - - - -                                 | 22 |
|      | B. $TE_{10}$ MODE LUNEBERG LENS - - - - -               | 25 |
|      | C. TEM MODE LUNEBERG LENS - - - - -                     | 26 |
| IV.  | CONCLUSIONS AND RECOMMENDATIONS - - - - -               | 43 |
|      | APPENDIX A: Ray Path Calculations - - - - -             | 46 |
|      | APPENDIX B: Electromagnetic Field Derivations - - - - - | 50 |
|      | APPENDIX C: Computer Programs - - - - -                 | 60 |
|      | BIBLIOGRAPHY - - - - -                                  | 72 |
|      | INITIAL DISTRIBUTION LIST - - - - -                     | 73 |
|      | FORM DD 1473 - - - - -                                  | 74 |



## LIST OF TABLES

| Table No.  | Page No. |
|--|----------|
| I. Theoretical and Experimental Curve Comparison ----- | 25       |



# LIST OF FIGURES

| Fig. No. |  | Page No. |
|----------|--|----------|
| 1.       | Focusing Properties of the Luneberg Lens -----   | 10       |
| 2.       | Geometry for Luneberg Lens Ray Path Derivation -----   | 12       |
| 3.       | Ray Paths through Luneberg Lens -----  | 14       |
| 4.       | Geometry for the Derivation of the Aperature Fields ----   | 15       |
| 5.       | Luneberg Lens Geometry Used in the Derivation of<br>Radiation Expressions -----                      | 19       |
| 6.       | Transmitter (X-Band) -----   | 23       |
| 7.       | Receiving/Pattern Recording System -----   | 24       |
| 8.       | Waveguide Feed Pattern and Luneberg Lens Aperature Field   | 28       |
| 9.       | Luneberg Lens Far Field Radiation Patterns with Wave-<br>guide Feed -----                            | 29       |
| 10.      | Luneberg Lens ( $TE_{10}$ mode) H-Plane Far Field Patterns<br>for Waveguide Feed -----               | 30       |
| 11.      | Luneberg Lens E-Plane Patterns for Waveguide Feed at<br>7.0 GHz -----                                | 31       |
| 12.      | Luneberg Lens E-Plane Patterns for Waveguide Feed at<br>8.0 GHz -----                                | 32       |
| 13.      | Luneberg Lens E-Plane Patterns for Waveguide Feed at<br>9.0 GHz -----                                | 33       |
| 14.      | Luneberg Lens E-Plane Patterns for Waveguide Feed at<br>10 GHz -----                                 | 34       |
| 15.      | Luneberg Lens E-Plane Patterns for Waveguide Feed at<br>11 GHz -----                                 | 35       |
| 16.      | Yagi Array Feed Pattern and Luneberg Lens Aperature<br>Field for Yagi Feed -----                     | 36       |
| 17.      | Luneberg Lens ( $TE_{10}$ mode) E-Plane Patterns for Yagi<br>Feed at 10 GHz -----                    | 37       |
| 18.      | TEM Mode Luneberg Lens Theoretical E-Plane Radiation<br>Patterns with Waveguide Feed at 10 GHz ----- | 38       |



|   |    |
|---|----|
| 19. Dielectric Loaded Sectoral Horn Feed Patterns and<br>Aperature Field for Sectoral Horn Feed -----       | 39 |
| 20. TEM Mode Luneberg Lens Theoretical E-Plane Radiation<br>Patterns for Sectoral Horn Feed at 10 GHz ----- | 40 |
| 21. TEM Mode Luneberg Lens Experimental E-Plane Pattern<br>for Sectoral Horn Feed at 10 GHz -----           | 41 |
| 22. TEM Mode Luneberg Lens H-Plane Radiation Patterns for<br>Sectoral Horn Feed at 10 GHz -----             | 42 |
| 23. Geometry for Luneberg Lens Ray Path Derivations -----   | 47 |
| 24. Luneberg Lens Geometry Used in the Derivation of<br>Radiation Expressions -----                         | 51 |



## I. INTRODUCTION

Theoretical work by R.K. Luneberg [Ref. 1] on optics in a medium of variable index of refraction resulted in the development of the Luneberg Lens which has many applications in microwave antennas. Two of the most common Luneberg Lenses are of the spherical and cylindrical types, in which the index of refractions is a function of radius only. In these lenses, the index of refraction is varied so that the radiation from a point source placed at the edge of the lens produces a collimated beam on the opposite side of the lens. The index of refraction is 1.0 at the edge of the lens so that it is matched to free space.

Spherical or cylindrical Luneberg Lenses are constructed by bonding concentric dielectric shells or hoops together, or by a special mixing and blending process which produces a continuously varying index of refraction as a function of the radius [Ref. 2]. Cylindrical lenses are also produced by taking a cylinder of dielectric material and machining one surface until the required average index of refraction, when placed between two parallel plates, is achieved.

Cylindrical Luneberg Lenses operate in either the TEM or the  $TE_{10}$  modes. If the thickness of the lens is greater than one-half wavelength but less than one wavelength, it operates in the  $TE_{10}$  mode. However, if the lens is several wavelengths thick it will operate in the TEM mode.

Many radar systems and most electronic warfare systems require antennas that can scan a narrow beam over wide angles in space. As long as the scan rates are low, the present rotating systems are adequate. However, when the required scan rates are increased or the application



requires instantaneous repositioning of the beam, rotating antennas cannot fulfill the requirements due to their inertia. It can be shown that for some passive electronic warfare systems the optimum scan rates are in excess of 3000 rpm. In addition to this, the beamwidth of present rotating antenna systems are too wide to permit the desired accuracy in the determination of the direction of arrival of an intercepted signal.

A new antenna system is therefore required to more fully utilize the capabilities of current equipment. The Luneberg Lens has the potential to overcome the above deficiencies and, in addition, provide a higher gain and reduce the weight of heavy antenna systems placed on the superstructure of ships. In view of this potential, this thesis was designed to analyze the parallel plate, continuously varying dielectric, cylindrical Luneberg Lens. The analysis was to produce theoretical expressions for the far field radiation patterns of the lens for any feed system. This would provide a method of determining the performance of any size lens with any feed system to be investigated without going to the expense of buying or constructing a lens and measuring the far field radiation patterns. The only requirement is that the radiation patterns of the feed system be known. The feed system patterns may be known functions or they may be measured. The far field expressions were programmed on the IBM 360 computer to compute and plot the far field radiation patterns. The accuracy of this analysis was verified experimentally.

Although the analysis of the Luneberg Lens was carried out for arbitrary feed polarization, lens size, and frequency, some limits had to be placed upon the experimentation. The experimental limitations were:

- (1) feed systems polarized in a plane perpendicular to the plane of the lens,
- (2) the far field radiation patterns of the feeds were used in



calculating the far field expressions of the Luneberg Lenses, (3) all the experimentation was confined to x-band due to availability of equipment, and (4) a "roof-top" range was used for some measurements.



## II. THEORETICAL ANALYSIS

Electromagnetic energy propagating through a lens follows optical ray paths [Ref. 3]. In the case of the radially-symmetric, cylindrical Luneberg Lens, the optical ray paths are such that the energy from an incident plane wave is focused into a cylindrical wave front on the surface of the lens diametrically opposite the direction of incidence as

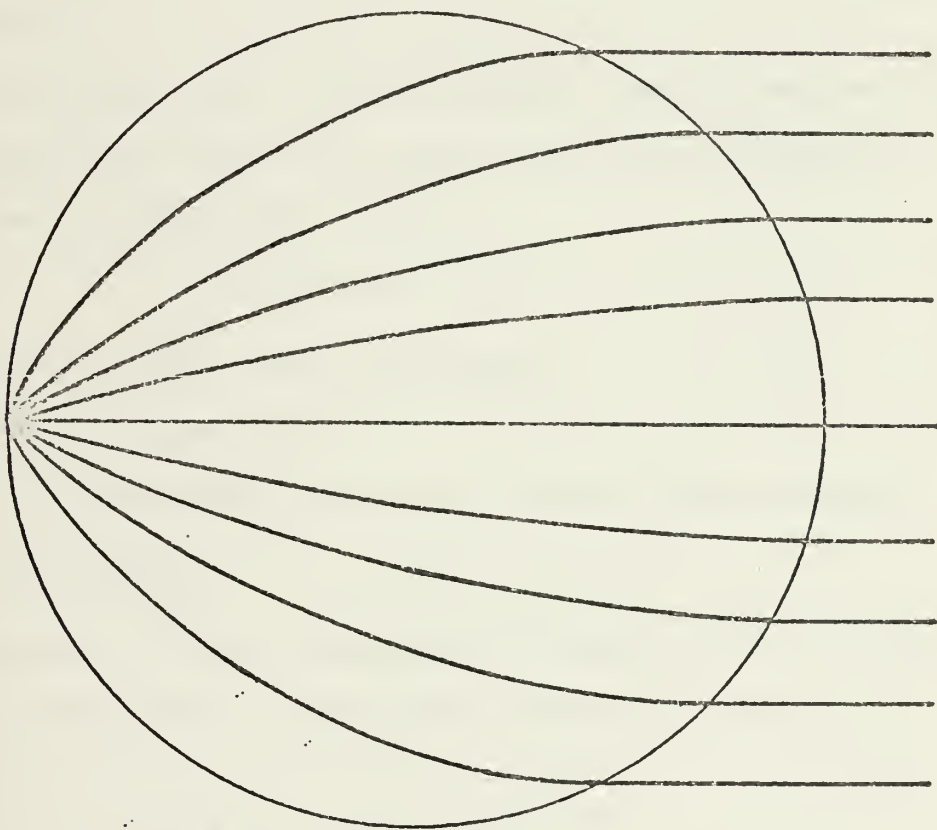


Figure 1. Focusing Properties of the Luneberg Lens.

indicated in Fig. 1.

The refraction necessary to achieve this focusing effect is obtained by properly varying the index of refraction. In the cylindrical Luneberg Lens the index of refraction,  $n(r)$  is given by

$$n(r) = \sqrt{2 - (r/r_0)^2}, \quad (1)$$



where  $r$  is any radius and  $r_0$  is the radius of the lens. Thus the index of refraction varies from  $\sqrt{2}$  at the center of the lens to 1.0 at the edge.

The theoretical analysis of the Luneberg Lens is based upon the principles of geometric optics from which the Ray Paths and the Aperature Field of the Lens are calculated and plotted. The far field radiation patterns are then calculated from the Aperature Field.

#### A. RAY PATHS

The generalized Snell's Law for circular symmetry, such as is present in the cylindrical Luneberg Lens, where the index of refraction is a function of the radius only [Ref. 3] is:

$$n(R) \sin \theta = C_1, \quad (2)$$

where  $n(R) = \sqrt{2-R^2}$  = index of refraction,

$R$  = normalized radius,

$\theta$  = angle between the ray path and the outward meridian,

$C_1$  = constant.

The geometry of Fig. 2 and equation (2) were utilized to derive an integral formula<sup>1</sup> for the relationship between  $R$ ,  $\Psi$ , and  $C_1$ .

$$\Psi = C_1 \int \frac{1}{R} [-R^4 + 2R^2 - C_1^2]^{-1/2} dR, \quad (3)$$

where  $\Psi$  is the angle between the direction of arrival of the plane wave and the radius through a point on the ray. A unique ray exists for each value of  $C_1$  ( $0.0 \leq C_1 \leq 1.0$ ).

---

<sup>1</sup> For complete derivation see Appendix A.



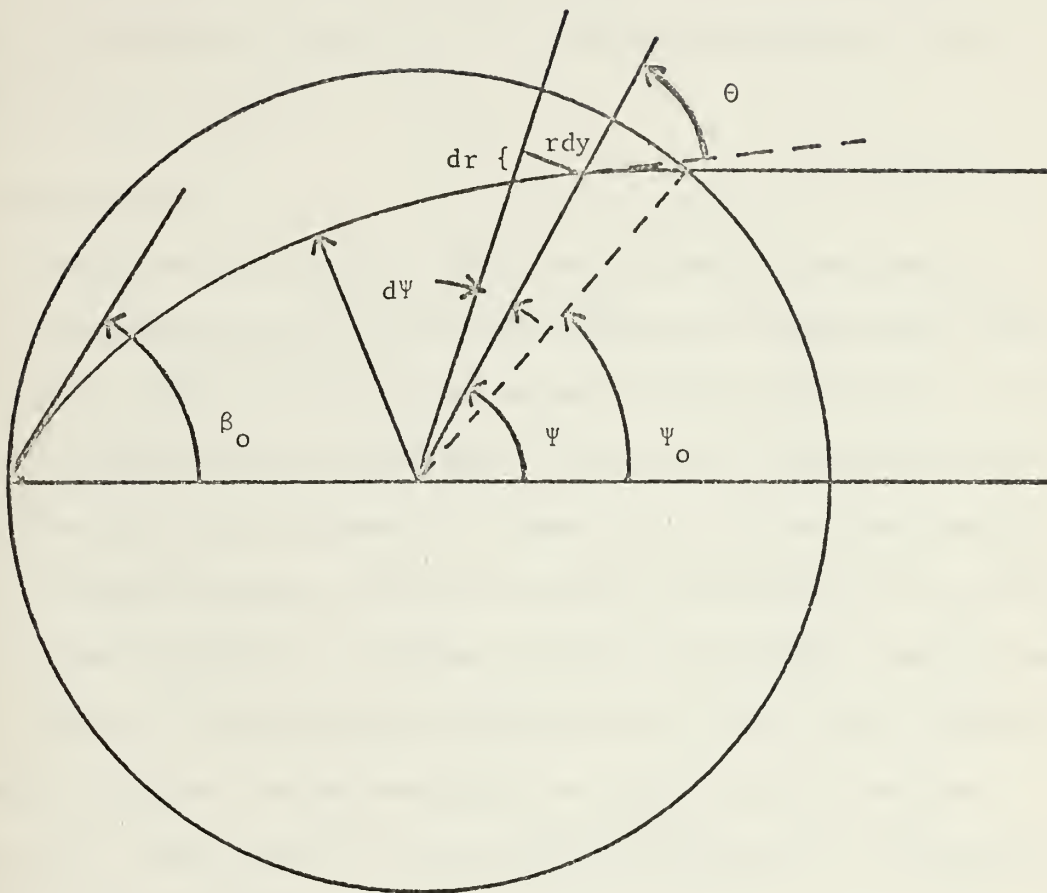


Figure 2. Geometry for Luneberg Lens Ray Path Derivation.



Equation (3) was separated into two intervals as given by equations (41) and (42) of Appendix A and programmed for the IBM 360 computer. The ray path plots are given in Fig. 3 for ten values of  $C_1$ . Note that  $\beta_0$  was equal to  $\psi_0$  and that the closest point of approach to the origin by a ray ( $r_m$ ) occurred for  $\theta$  equal to  $90^\circ$ . Each ray is symmetric about the point ( $r = r_m$ ,  $\theta = 90^\circ$ ).

#### B. APERATURE FIELD

The relationship between the Feed Distribution and the Aperature Field of the Luneberg Lens was derived utilizing the principles of geometric optics, for the geometry and variables defined in Figure 4. The energy flow into a Differential Element  $d\beta dx$  must be identical to the energy flow out of the Differential Element  $dx dy$ , since from the principles of Geometric Optics it has been shown in section II-A that energy flow is along Ray Paths. If a tube of rays is considered, then the energy flow is constant through various cross-sections of the tube. Therefore, the energy flow into the wedge-shaped tube,  $d\beta dx$ , at the feed is  $S_1(\beta, x) d\beta dx$ , where  $S_1(\beta, x)$  is the energy distribution per unit angle in the primary feed pattern.

Equating the energy that enters the flux tube,  $d\beta dx$ , to the energy leaving the flux tube,  $dx dy$ ,  $S_a(x, y) dx dy = S_1(x, \beta) d\beta dx$ , where  $S_a(x, y)$  is the energy in the lens aperature. However,  $S_a(x, y)$  is proportional to  $|E'_a|^2$ , where  $|E'_a|$  is the magnitude of the electric field in the aperature. Therefore,

$$S_a(x, y) dx dy = C_2 |E'_a|^2 dx dy = S_1(x, \beta) d\beta dx \quad (4)$$

where  $C_2$  is a constant. From the geometry of Figure 4

$$y = r_0 \sin \psi \quad (5)$$



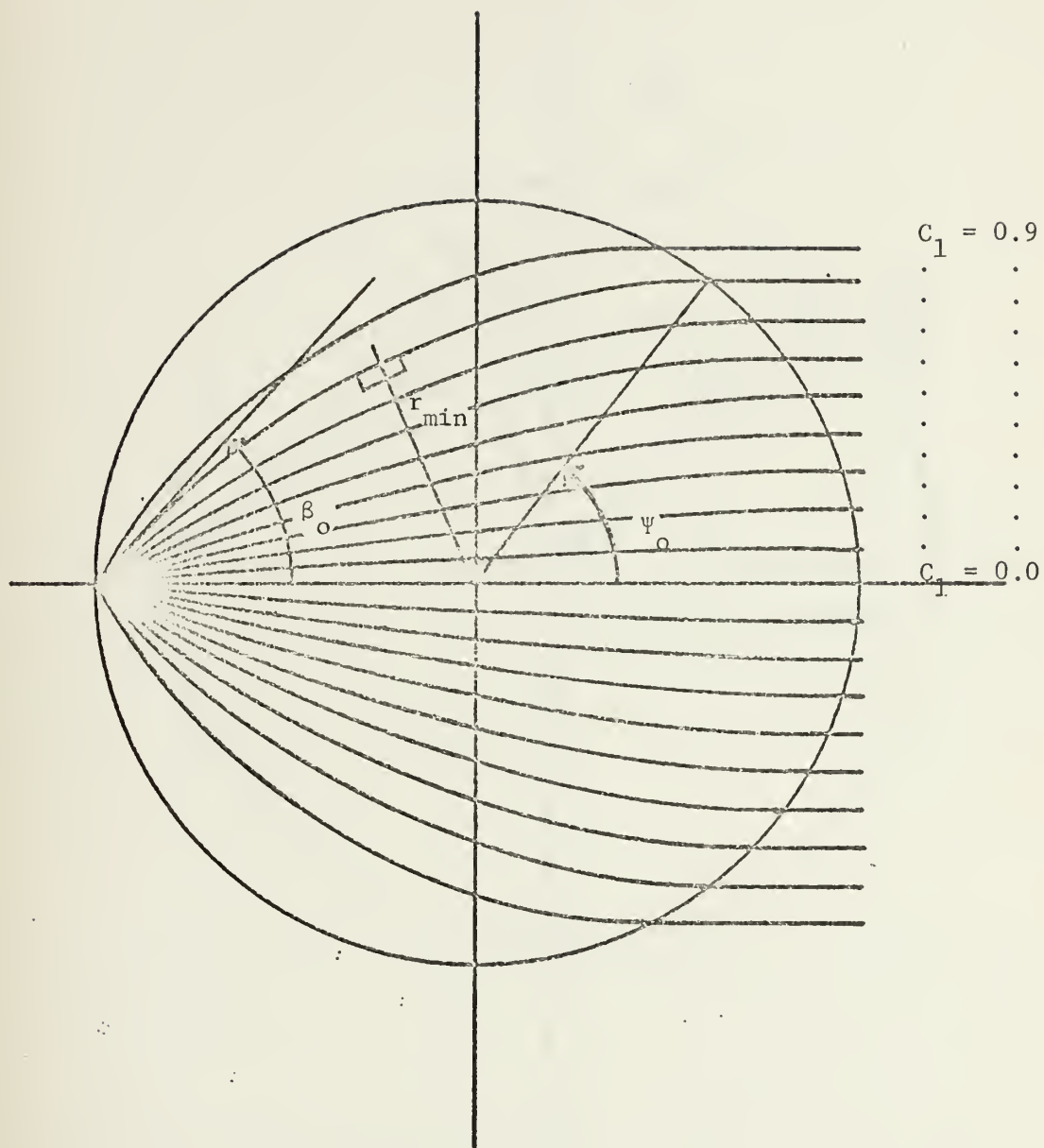


Figure 3. Ray Paths Through Luneberg Lens.



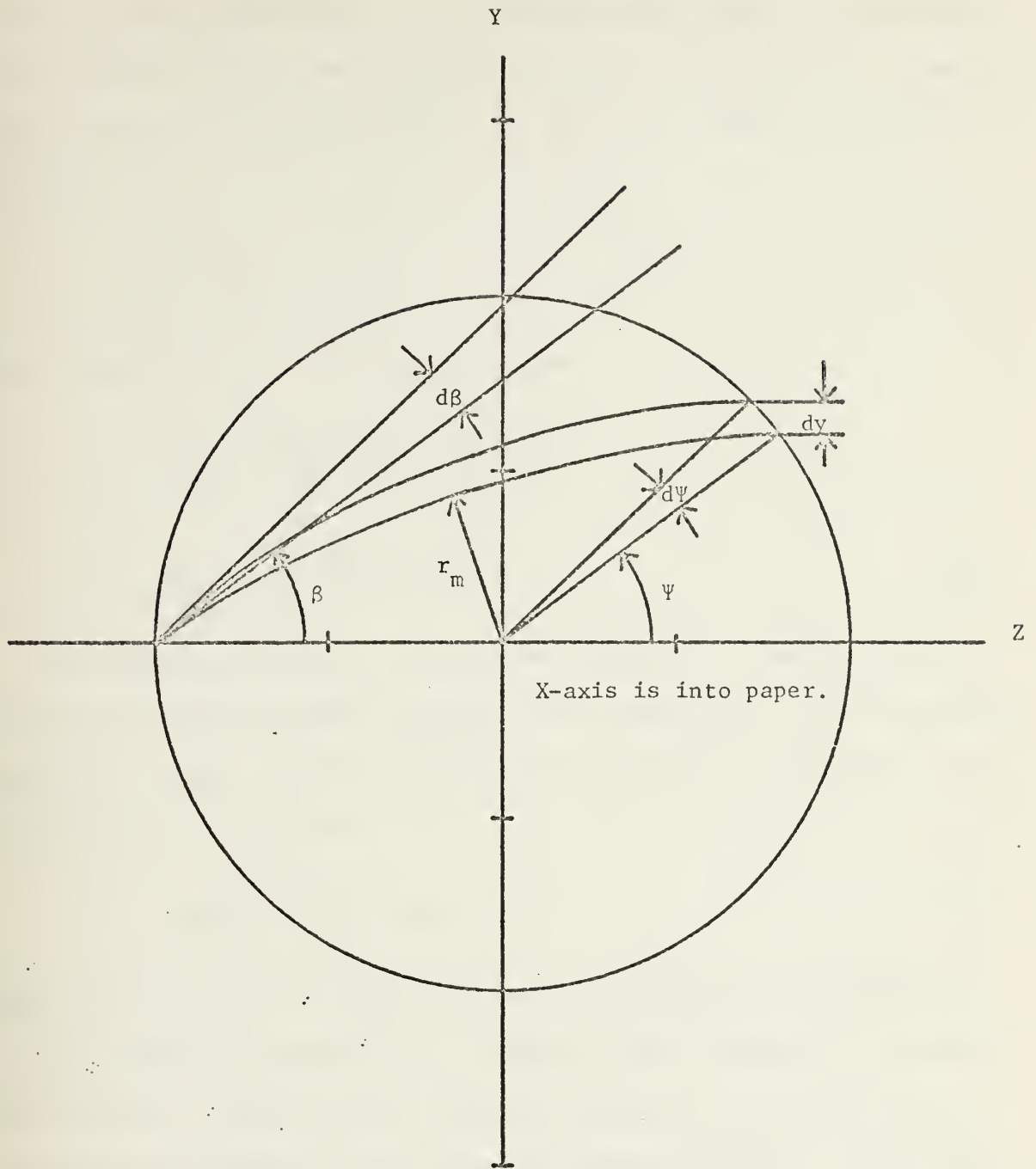


Figure 4. Geometry for the Derivation of the Aperture Fields.



where  $r_o$  is the lens radius.  $r_m$  is defined as the point on a ray nearest the origin, and due to the symmetry of the Lens, the ray path is symmetric about the point  $r = r_m$  and hence  $\Psi = \beta$  [Ref. 4]. Then from equation (5) and this fact

$$\frac{dy}{d\Psi} = \frac{dy}{d\beta} = r_o \cos \Psi.$$

Substituting this into equation (4) yields

$$|E'_a|^2 = \frac{S_1(x, \beta)}{C_2} \frac{d\beta}{dy} = \frac{S_1(x, \Psi)}{C_2 r_o \cos \Psi}$$

or

$$|E'_a| = C_3 \sqrt{S_1(x, \Psi) \sec \Psi} \quad (6)$$

The Aperture field can therefore be calculated for any feed distribution for either the TEM or the  $TE_{10}$  mode Luneberg Lens. Two assumptions were made. First, that the feed energy distribution is a separable function of  $x$  and  $\Psi$ . Therefore

$$S_1(x, \Psi) = S_2(x) S_3(\Psi). \quad (7)$$

The second assumption is that  $S_2(x)$  and  $S_3(\Psi)$  can be calculated or approximated from the geometry or by computer curve fitting of a measured feed pattern. For either type Luneberg Lens the  $S_3(\Psi)$  can be equated to the feed distribution in the plane of the lens [Ref. 4].  $S_2(x)$ , however, is different for each type of lens and is a function of the lens geometry. In the  $TE_{10}$  mode lens as is suggested from wave guide theory

$$[S_2(x)]_{TE_{10}} \propto \cos\left(\frac{x}{a}\right), \quad (8)$$

where  $a$  is the thickness of the lens. In the TEM mode lens the assumption



was made that the  $S_2(x)$  is constant over the x-dimension of the lens, and

$$[S_2(x)]_{\text{TEM}} \propto C_4. \quad (9)$$

The Luneberg Lens was designed to produce a constant phase in the plane of the lens along a line tangent to the aperture center; therefore, the aperture fields have a phasing

$$kr_0(1 - \cos \Psi). \quad (10)$$

Then for the Luneberg Lens

$$E'_a = |E'_a| e^{jkr_0(1 - \cos \Psi)}. \quad (11)$$

Combining equations (6), (7), and (9) for the TEM mode Luneberg Lens,

$$E'_a \propto \sqrt{S_3(\Psi) \sec \Psi}. \quad (12)$$

However,  $S_3(\Psi) \propto (E'_a(\Psi))^2$ , so that

$$E'_a(x, \Psi) = C_5 E_a(\Psi) \sqrt{\sec \Psi}, \quad (13)$$

where  $C_5$  is a constant of proportionality and  $E_a(\Psi)$  is the magnitude of the feed distribution. Rewriting with the phasing information of equation (10),

$$E'_a(x, \Psi) = C_5 E_a(\Psi) \sqrt{\sec \Psi} e^{jkr_0(1 - \cos \Psi)}. \quad (14)$$

Combining equations (6), (7), and (8) for the  $TE_{10}$  mode Luneberg Lens the aperture field is

$$E'_a \propto |E'_a| \sqrt{S_3(\Psi) \sec \Psi} \cos\left(\frac{x}{a}\right)$$

or

$$E'_a(x, \Psi) = C_6 \cos\left(\frac{x}{a}\right) E_a(\Psi) \sqrt{\sec \Psi} e^{jkr_0(1 - \cos \Psi)}. \quad (15)$$



### C. ELECTROMAGNETIC FIELD CALCULATIONS

The Electric Field of the Luneberg Lens was calculated utilizing the aperture field method and Huygens Principle as developed in Chapter 2 of Ref. 5. The Electric Field equations are:

$$\overline{E} = -\frac{1}{\epsilon} \overline{\nabla} \times \overline{F} - \frac{j}{\omega\mu\epsilon} \overline{\nabla} \times \overline{\nabla} \times \overline{A}, \quad (16a)$$

and 
$$\overline{H} = \frac{1}{\mu} \overline{\nabla} \times \overline{A} - \frac{j}{\omega\mu\epsilon} \overline{\nabla} \times \overline{\nabla} \times \overline{F} \quad (16b)$$

where 
$$\overline{A} = \frac{\mu}{4\pi} \iiint \overline{J}(x', \psi') \frac{e^{-jkR}}{R} dS' , \quad (17)$$

$$\overline{F} = \frac{\epsilon}{4\pi} \iiint \overline{K}(x', \psi') \frac{e^{-jkR}}{R} dS' , \quad (18)$$

$$\overline{J}(x', \psi') = \overline{n} \times \overline{H}_a , \quad (19)$$

$$\overline{K}(x', \psi') = \overline{E}_a \times \overline{n} , \quad (20)$$

$$dS' = \rho dx' d\psi' , \quad (21)$$

$$k = \frac{2\pi}{\lambda} , \quad (22)$$

and the remaining variables are shown in Fig. 5. Only the Electric Field will be considered from this point since the Far-Field is essentially a plane wave, where E and H are related by the intrinsic impedance of Free-Space.

The Far-Field equations<sup>2</sup> derived from equations (16-22) and the geometry of Fig. 5 for a feed polarized in the x-direction are:

---

<sup>2</sup>See Appendix B for derivation.



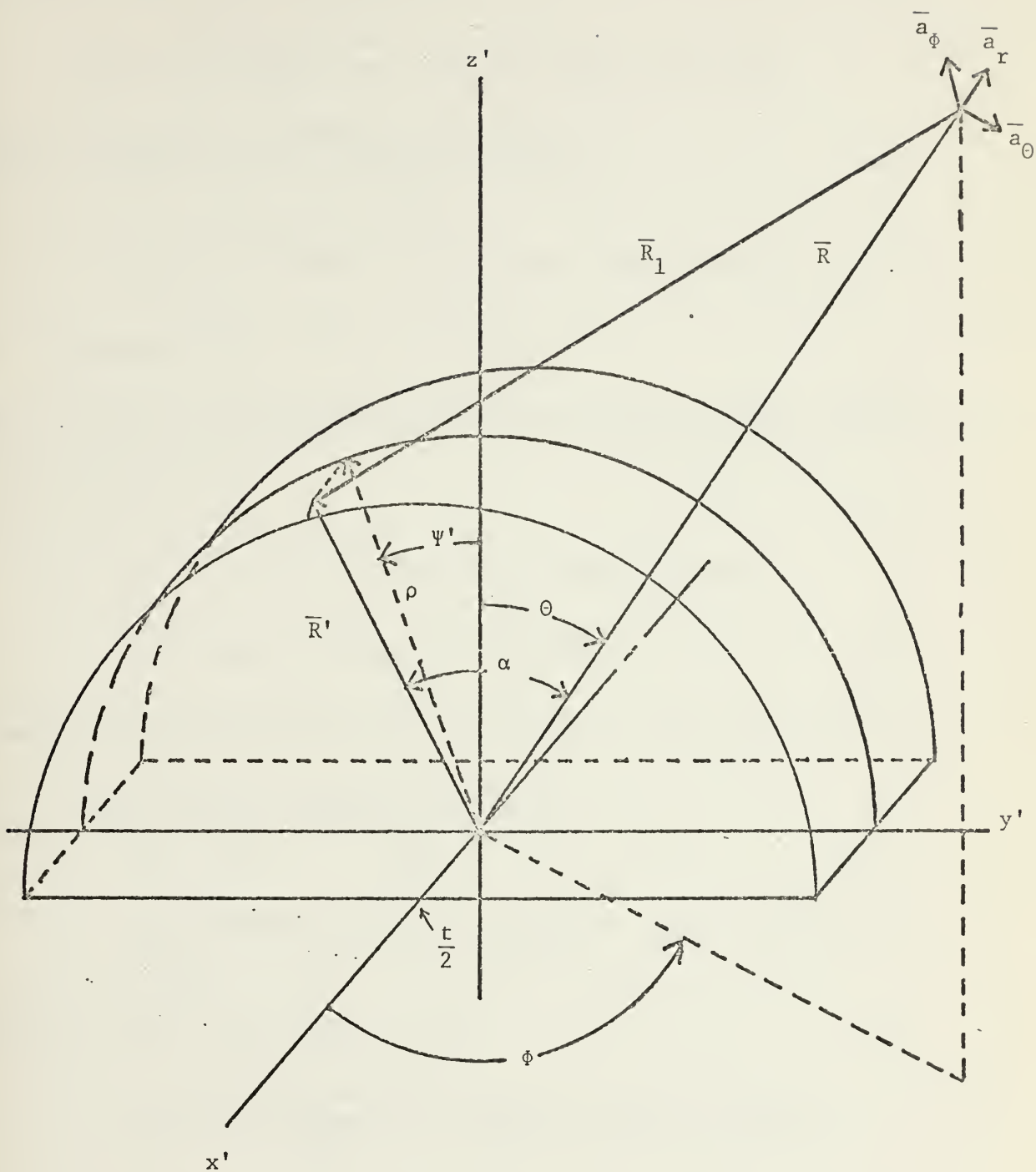


Figure 5. Luneberg Lens Geometry Used in the Derivation of Radiation Expressions.



$$\overline{E}_\Theta(R, \phi, \Theta) = \frac{jk\rho e^{jk\rho}}{4\pi} [1 - \cos \Theta][\cos \phi] \quad (23)$$

$$\iint \left[ \frac{e^{-jk|R_1|}}{|R_1|} \frac{e^{-jk\rho \cos \Psi'}}{|R_1|} \right] [E_{ax}(x', \Psi') \cos \Psi'] dx' d\Psi',$$

$$E_\Phi(R, \phi, \Theta) = \frac{jk\rho e^{jk\rho}}{4\pi} \iint \left[ \frac{e^{-jk|R_1|}}{|R_1|} \frac{e^{-jk\rho \cos \Psi'}}{|R_1|} \right] \quad (24)$$

$$[E_{ax}(x', \Psi')][\sin \Theta \sin \Psi' - \cos \Psi' \sin \phi(1 + \cos \Theta)] dx' d\Psi',$$

$$\text{and } E_R(R, \phi, \Theta) = 0; \quad (25)$$

where  $E_{ax}(x', \Psi)$  is the magnitude of the Lens aperture field polarized in the x-direction and

$$R_1^2 = [R^2 + (x')^2 + \rho^2 + 2R(x' \cos \Theta \cos \phi - \rho \sin \Psi' \sin \Theta \sin \phi + \rho \cos \Psi' \cos \Theta)]^{1/2}. \quad (26)$$

The far-field equations for a feed polarized in the y-direction are:

$$\overline{E}(R, \phi, \Theta) = \frac{jk\rho e^{jk\rho}}{4\pi} \iint \left[ \frac{e^{-jk|R_1|}}{|R_1|} \frac{e^{-jk\rho \cos \Psi'}}{|R_1|} \right] \quad (27)$$

$$[E_{ay}(x', \Psi')][\cos \Psi' \sin \phi (1 + \cos \Theta) - \sin \Theta \sin \Psi'] dx' d\Psi',$$

$$E(R, \phi, \Theta) = \frac{jk\rho e^{jk\rho}}{4\pi} [\cos \phi (\cos \Theta + 1)] \quad (28)$$

$$\iint \left[ \frac{e^{-jk|R_1|}}{|R_1|} \frac{e^{-jk\rho \cos \Psi'}}{|R_1|} \right] [E_{ay}(x', \Psi') \cos \Psi'] dx' d\Psi',$$

$$\text{and } E_R(R, \phi, \Theta) = 0; \quad (29)$$

where  $E_{ay}(x', \Psi')$  is the magnitude of aperture field polarized in the y-direction and  $|R_1|$  is as given in equation (26).



The Far-Field radiation patterns are identical as can be seen by comparing equations (23) and (24) to equations (28) and (27) respectively. Due to this identity, the Far-Field radiation patterns are independent of the Feed Polarization. Therefore, only one set of equations need be utilized in calculating and plotting the far-field radiation patterns for any feed polarization in the x-y plane.

Approximating  $\frac{1}{|\bar{R}_1|}$  by  $\frac{1}{|\bar{R}|}$  and  $|\bar{R}_1|$  by  $|\bar{R}| - |\bar{R}' \cdot \bar{a}_r|$  (far field condition)<sup>3</sup> then equations (13) and (14) become:

$$E_{\theta} = \frac{jk\rho}{4\pi R} [1 - \cos \theta] [\cos \phi] e^{jk(\rho-R)} \int e^{CEX} E_{a_1}(x) dx \int e^{CER} \cos \psi E_{a_1}(\psi) d\psi$$

(30)

$$E_{\phi} = \frac{jk\rho}{4\pi R} e^{jk(\rho-R)} \int e^{CEX} E_{a_1}(x) dx \int e^{CER} \cos \psi E_{a_1}(\psi)$$

$$[ \sin \theta \sin \psi - \cos \theta \sin \phi \cos \psi - \sin \phi \cos \psi ] d\psi , \quad (31)$$

$$\text{where} \quad CEX = jkx \sin \theta \cos \phi \quad (32)$$

$$\text{and} \quad CER = jk\rho(\cos \psi \cos \theta - \sin \psi \sin \theta \sin \phi - \cos \psi). \quad (33)$$

Equations (30) and (31) were programmed for the IBM-360 computer for calculating and plotting the normalized far-field radiation patterns. The computer programs are given in Appendix C, and the theoretical far-field radiation patterns are given in Section III.

---

<sup>3</sup>Calculations show that for the worst condition ( $\psi = 90^\circ$ ) at a distance of  $2L^2/\lambda$  the phasing error is less than  $.06\lambda$ , ( $21^\circ$ ).



### III. EXPERIMENTAL VERIFICATION

#### A. DISCUSSION

Experimental verification was undertaken to determine the validity of the equations that describe the far-field radiation patterns of the Parallel-Plate Luneberg Lenses. In order to accomplish this, two Luneberg Lenses were acquired. One was a TEM mode lens, 44 inches ( $37.2 \lambda$  at 10 GHz) in diameter and 2.38 inches thick. The other was a  $TE_{10}$  mode lens, 10.25 inches ( $8.67\lambda$  at 10 GHz) in diameter and 0.5 inches thick. All measurements were made with the lenses operating in the receive mode and for far-field conditions (distance  $> 2L^2/\lambda$ ). Measurements on the  $TE_{10}$  mode lens were conducted in an anechoic chamber and those for the TEM mode lens were conducted in a "roof-top" range. The transmitting set-up is shown in Fig. 6, and was operated in the CW mode at 10 GHz. The only exception was for a frequency characteristics check of the  $TE_{10}$  mode lens. The receiving set-up is given in Fig. 7.

The procedure followed was to measure the far-field patterns of the feed and the Luneberg Lens and then using the feed data, calculate the far-field patterns and compare the two results.

It was noted that in the case of all feeds with both lenses that when the feed was placed very close to the lens the first side lobes almost merged into the main beam. As the distance between the feed and lens increased the side lobes became distinct and dropped very rapidly. Then the particular placement of the feed was found which resulted in optimum (lowest) side lobe levels. When the separation was increased to a distance greater than the optimum, the main beam spread out and engulfed the first side lobes.



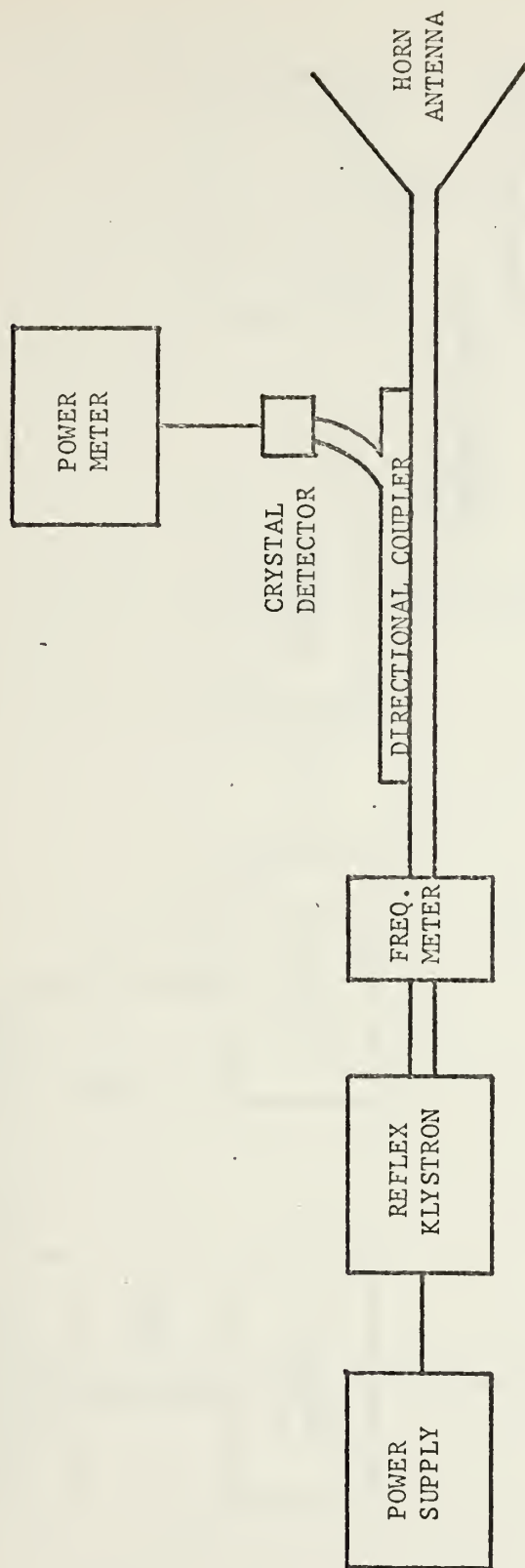


Figure 6. Transmitter (X-Band).



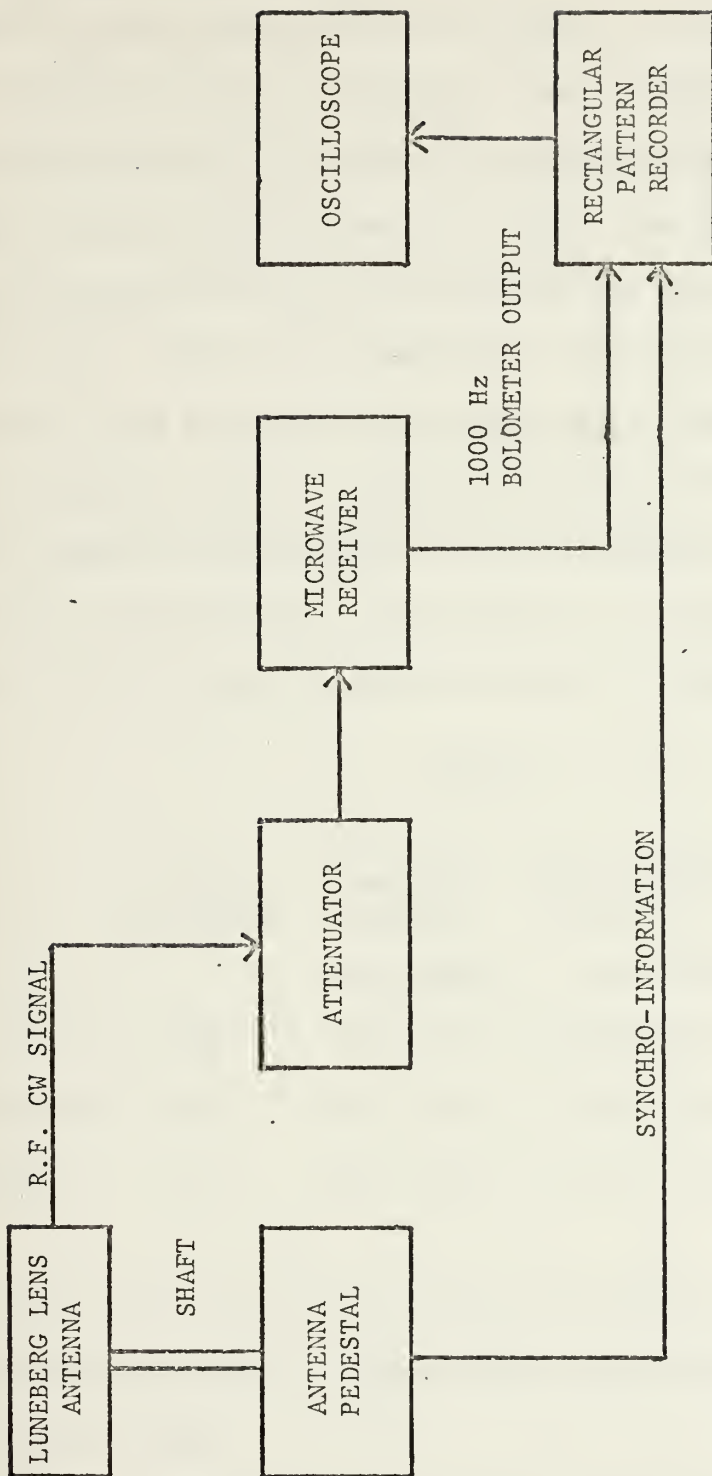


Figure 7. Receiving/Pattern Recording System.



## B. $TE_{10}$ MODE LUNEBERG LENS

The  $TE_{10}$  Mode Luneberg Lens was fed by two different feed systems. The first was an "open-end" waveguide feed (hereafter referred to as the waveguide feed) and the other was a two element Yagi array (driven element plus director) resonant at 10 GHz. The far field patterns of the lens aperture fields for these feeds are given in Figures 8 and 16 respectively. Fig. 9 is a comparison of the theoretical vs. the experimental far field patterns in the planes of the lens (E-plane), when fed by the waveguide feed at a frequency of 10 GHz. The gain over isotropic of this system is approximately 20 db, as compared to a 16 db standard horn, with a one-half power beam width of 6.5 degrees. The salient points of the two curves are given in Table I, below.

TABLE I

|              | 3 db<br>Beam Width | First Null<br>Location |       | First Sidelobe<br>Location |       | First Sidelobe<br>Amplitude (db) |       |
|--------------|--------------------|------------------------|-------|----------------------------|-------|----------------------------------|-------|
|              |                    | left                   | right | left                       | right | left                             | right |
| Theoretical  | 6.8°               | -8.2°                  | 8.3°  | -10.8°                     | 10.6° | -19.6                            | -19.6 |
| Experimental | 6.5°               | -7.4°                  | 7.8°  | -9.9°                      | 10.3° | -17.9                            | -18.2 |
| Difference   | 0.3°               | 0.6°                   | 0.5°  | 0.9°                       | 0.3°  | 1.7                              | 1.4   |

Figure 10 is a comparison of the theoretical and experimental H-plane (perpendicular to plane of lens at beam center) far field patterns for the waveguide feed.

In order to determine the frequency characteristics of the  $TE_{10}$  mode lens when fed by the waveguide, feed far field patterns for 7, 8, 9 and 11 GHz were also calculated and are presented in Figures 11 and 15. The



experimental far field patterns were different from the theoretical patterns by about the same amount as the patterns at 10 GHz.

The experimental vs. theoretical E-plane far field patterns of the  $TE_{10}$  Mode Lens fed by the Yagi feed are given in Fig. 17. The differences in side lobe and null locations and side lobe levels are negligible. The gain over isotropic of this arrangement is about 21.5 db as compared to the 16 db standard gain horn, with a one-half power beam width of 6.2 degrees.

A comparison of the lens aperture fields ( Figures 8 and 16) show that the Yagi array feed utilizes the lens aperture more efficiently than the waveguide feed.

#### C. TEM MODE LUNEBERG LENS

The theoretical and experimental E-plane far field patterns of the TEM Mode Luneberg Lens when fed with a dielectrically loaded sectoral horn feed (feed pattern and lens aperture field given in Fig. 19) are given in Figures 20 and 21, respectively. The difference between these two patterns is about 1.0 degrees in the one-half power beam width, 0.5 degrees in the first null placement, 2.5 degrees in the first sidelobe placement, and 8.0 db in first sidelobe amplitudes. The gain over isotropic of this arrangement was about 25 db. The theoretical H-plane far field pattern is given in Fig. 22. The 3 db theoretical H-plane beam width is 22 degrees as compared to 25.5 degrees obtained experimentally by the Naval Electronic Laboratory Center [Ref. 2].

When the TEM mode lens was fed by the waveguide feed (Fig. 8) the theoretical (Fig. 18) and the experimental far field pattern differences were somewhat less than they were for the sectoral horn, but due to range difficulties reliable experimental patterns were not obtained.



It is felt that the differences between the theoretical and experimental patterns were too great to warrant further investigation without refinement of the feed systems analysis.



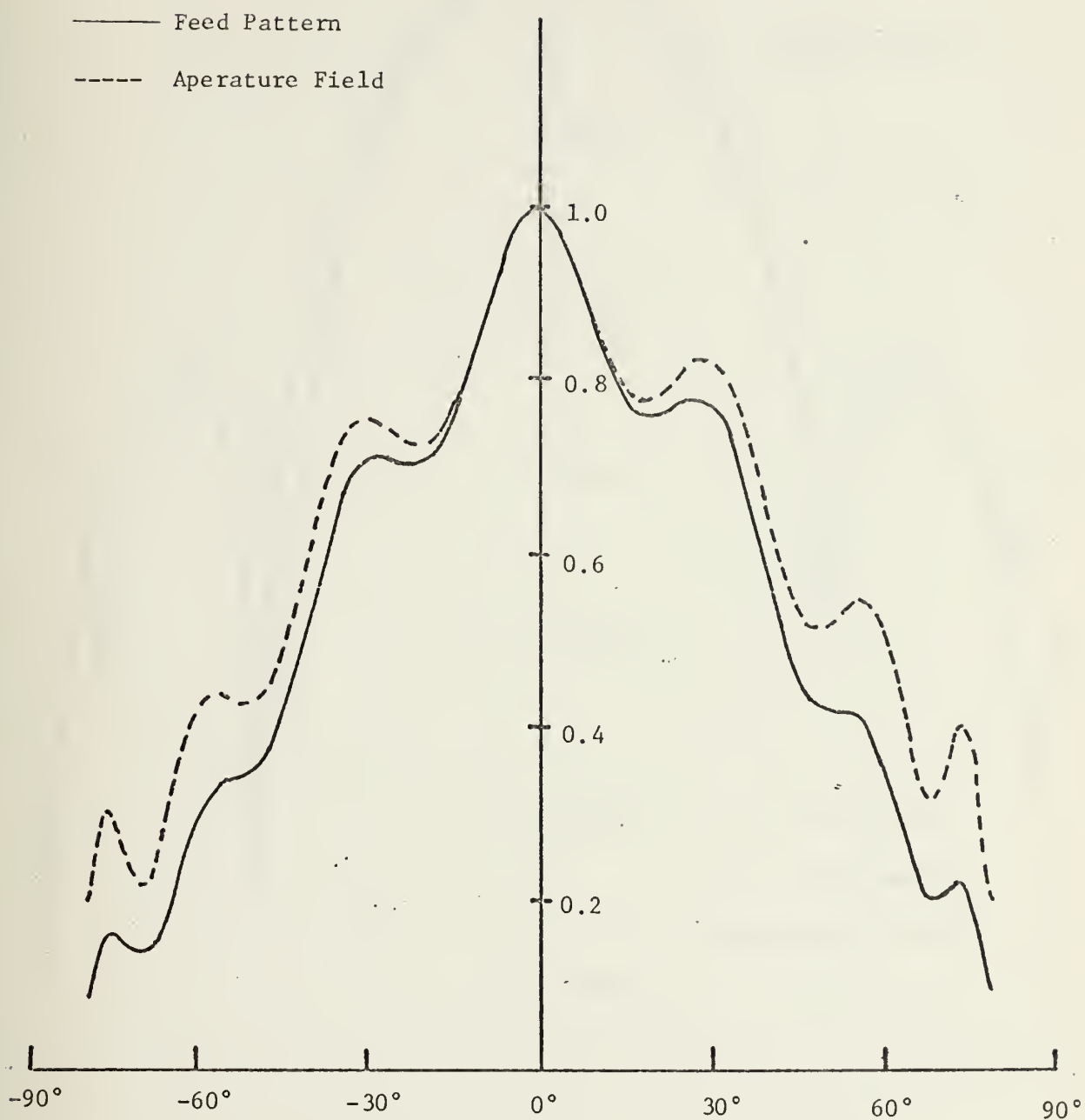


Figure 8. Waveguide Feed Pattern and Luneberg Lens Aperature Field.



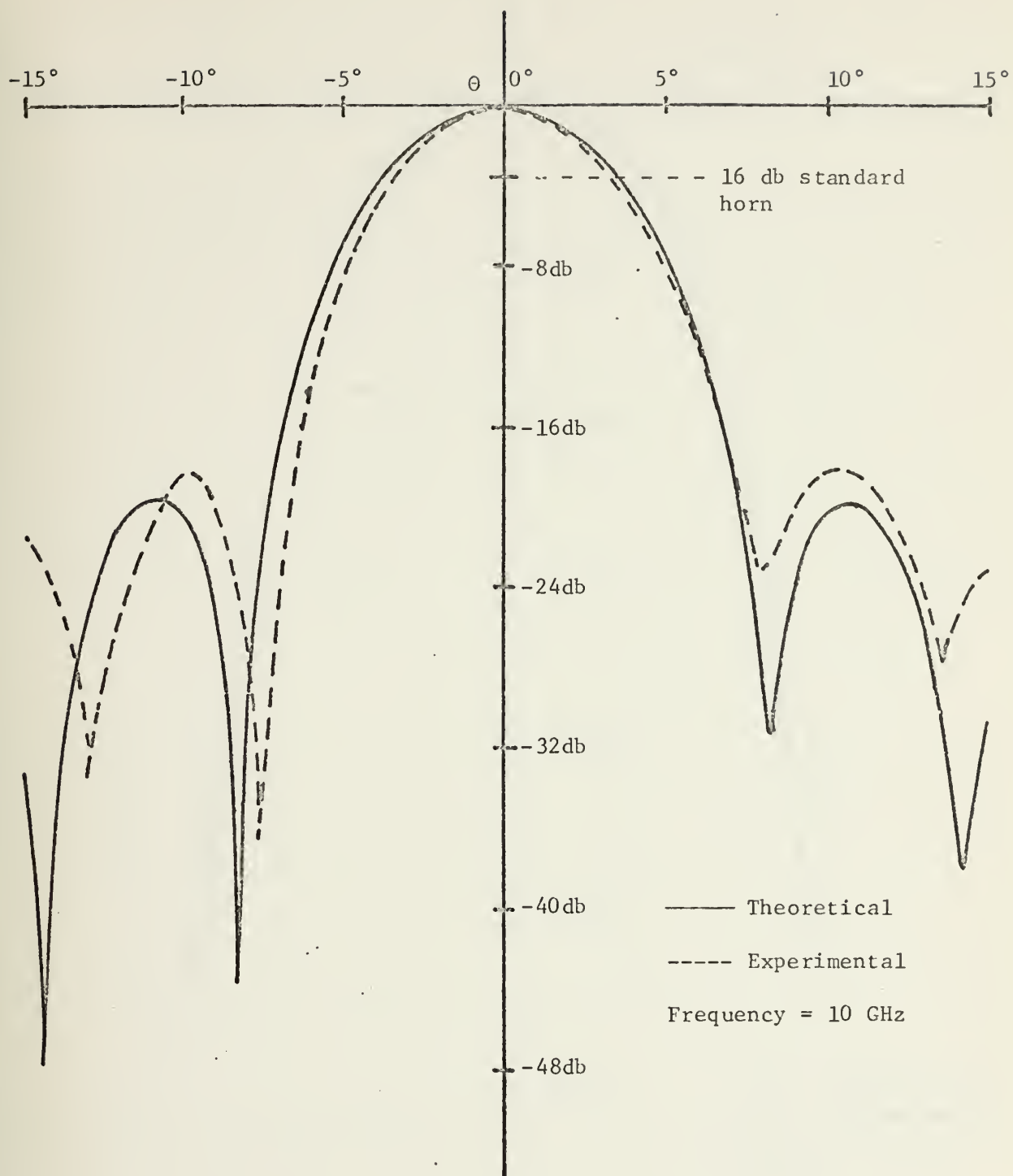


Figure 9. Luneberg Lens Far Field Radiation Patterns with Waveguide Feed.



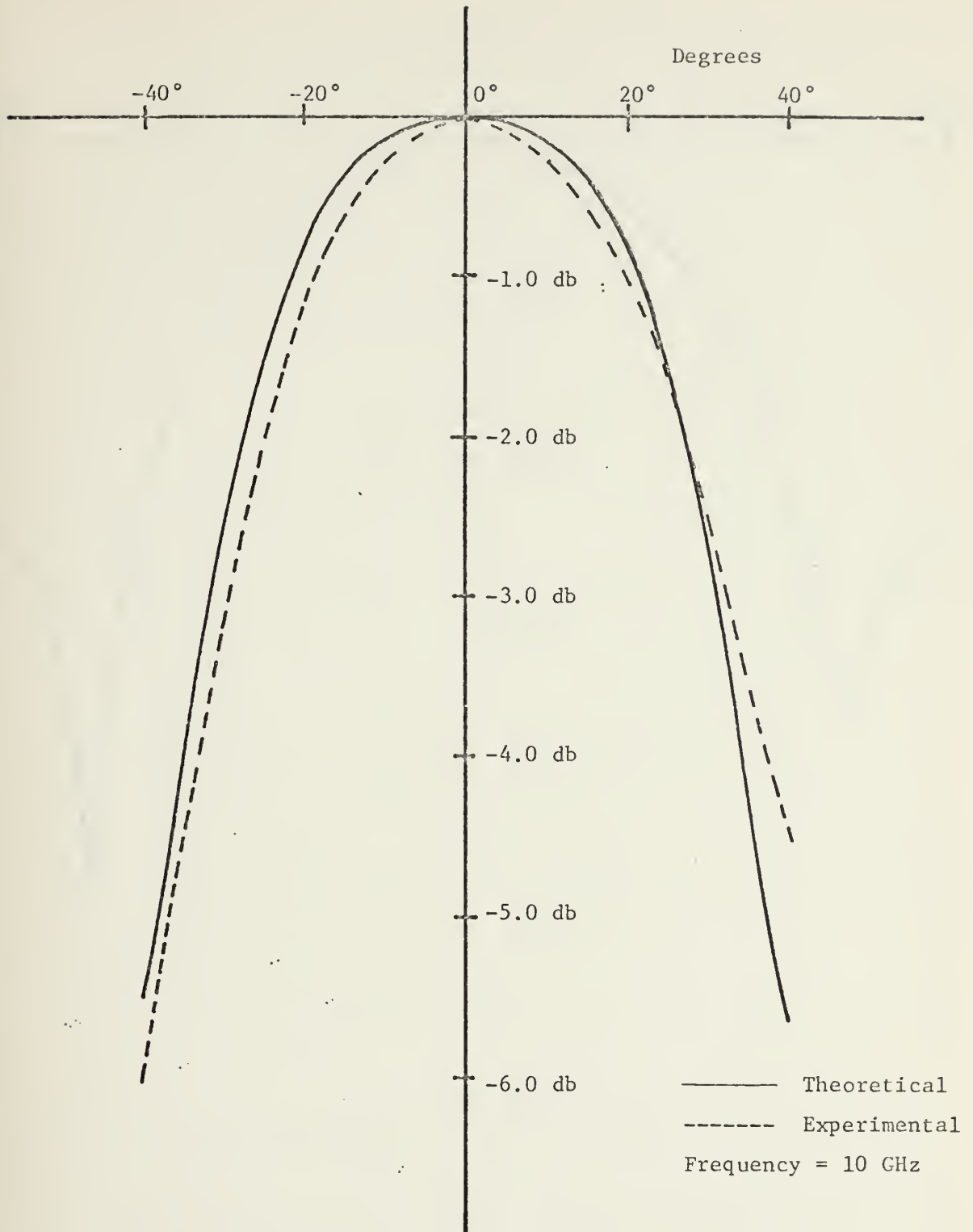


Figure 10. Luneberg Lens ( $TE_{10}$  mode) H-plane Far Field Patterns for Waveguide Feed.



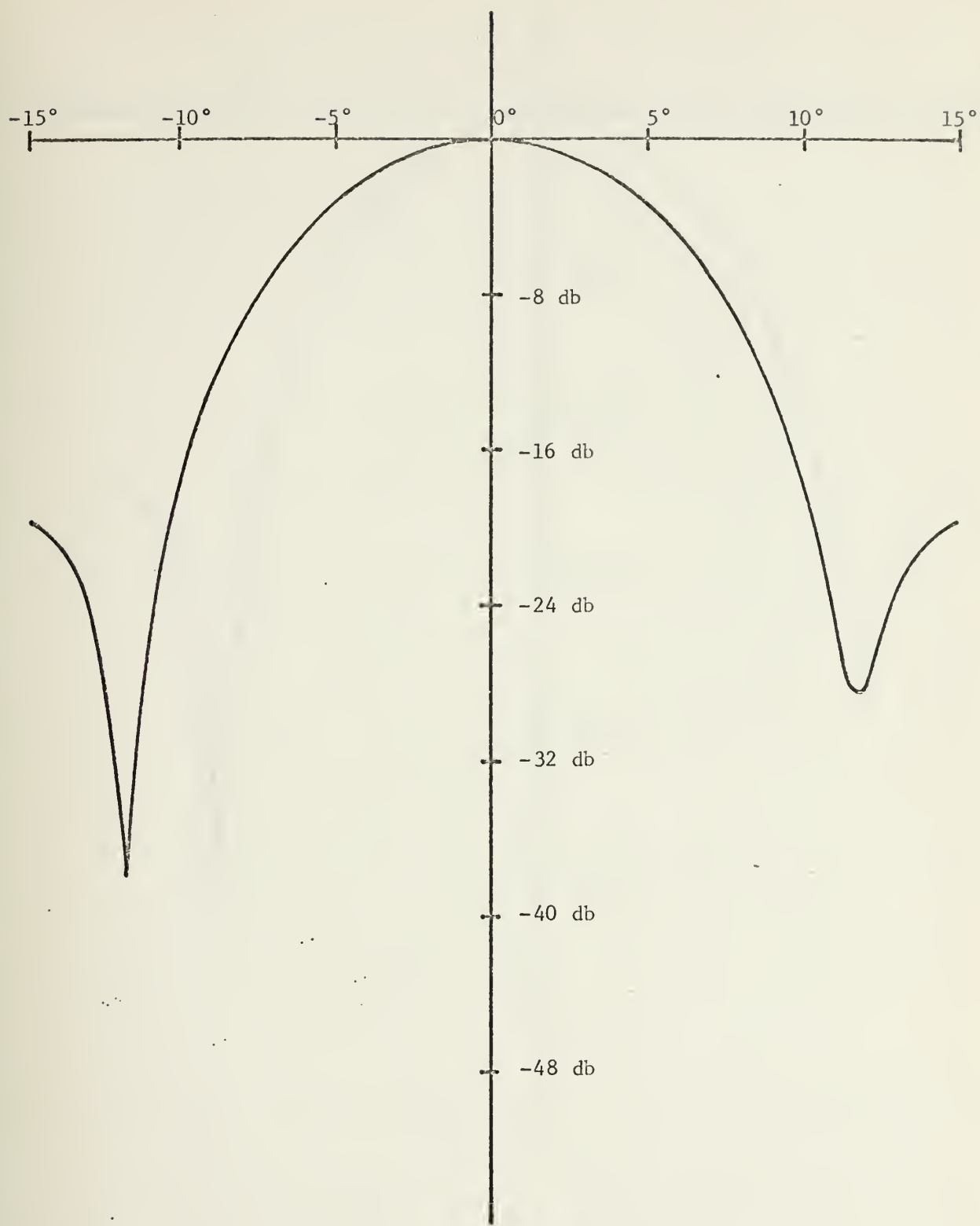


Figure 11. Luneberg Lens E-Plane Patterns for Waveguide Feed at 7.0 GHz.



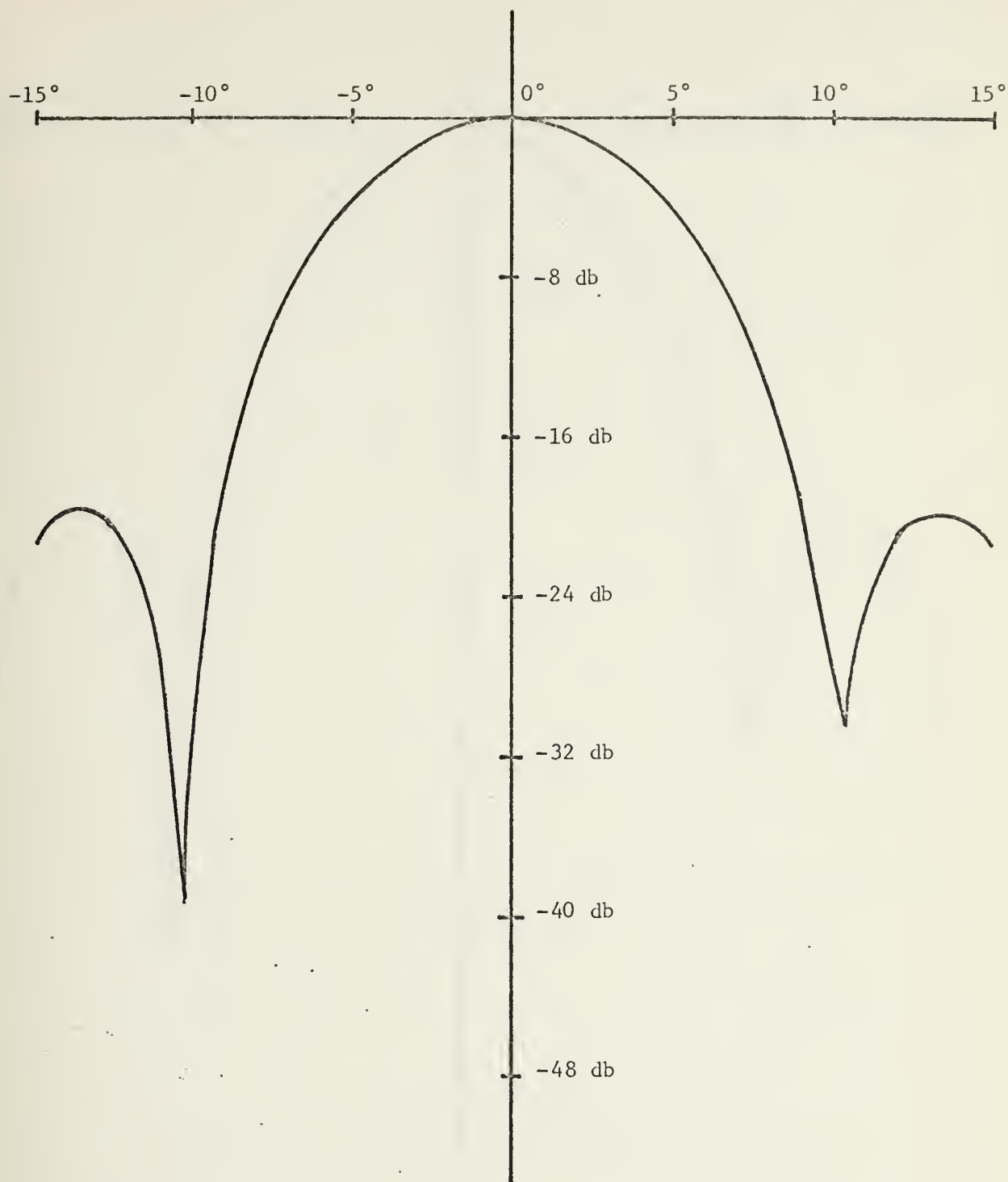


Figure 12. Luneberg Lens E-Plane Patterns for Waveguide Feed at 8.0 GHz.



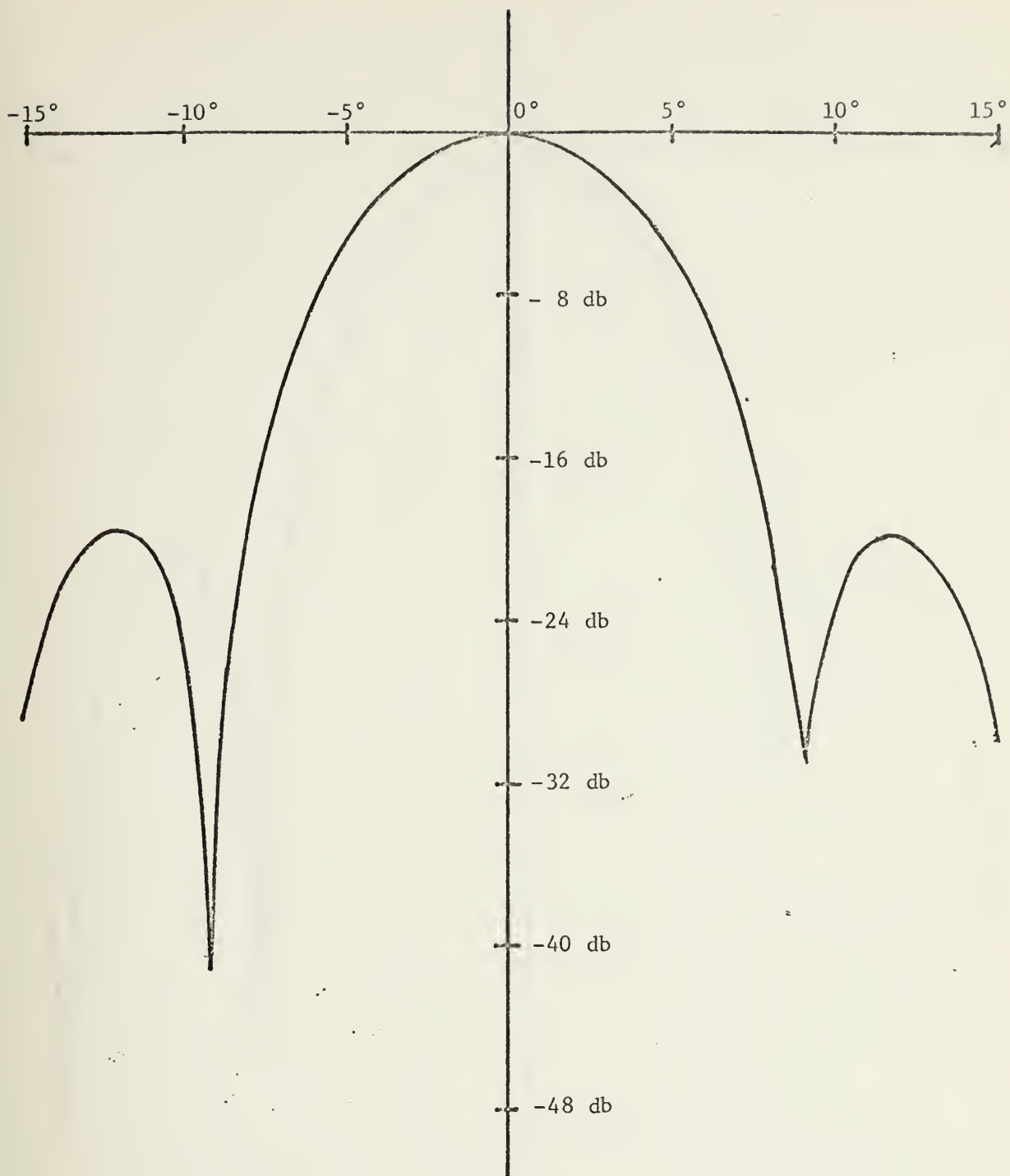


Figure 13. Luneberg Lens E-Plane Patterns for Waveguide Feed at 9.0 GHz.



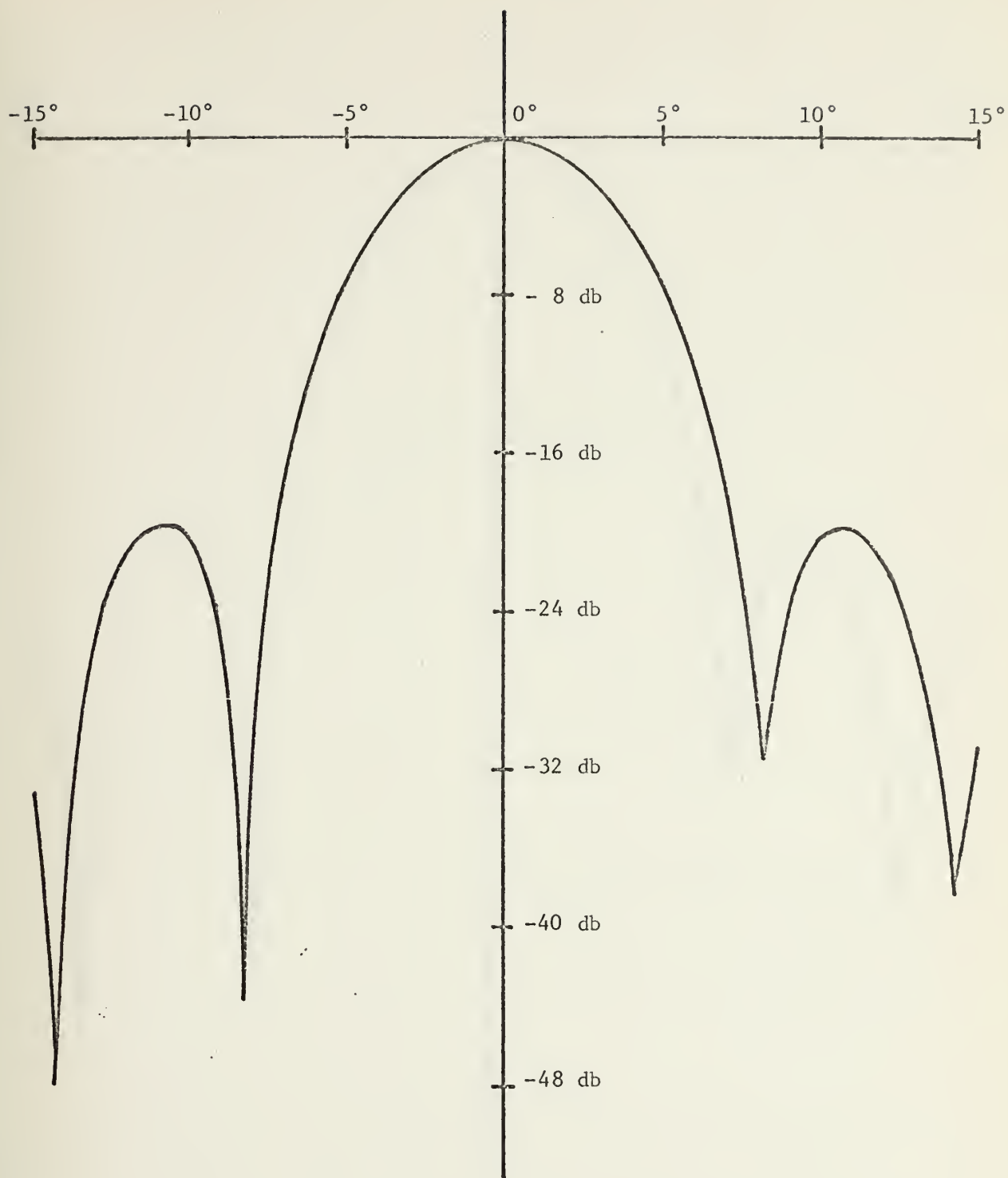


Figure 14. Luneberg Lens E-Plane Patterns for Waveguide Feed at 10 GHz.



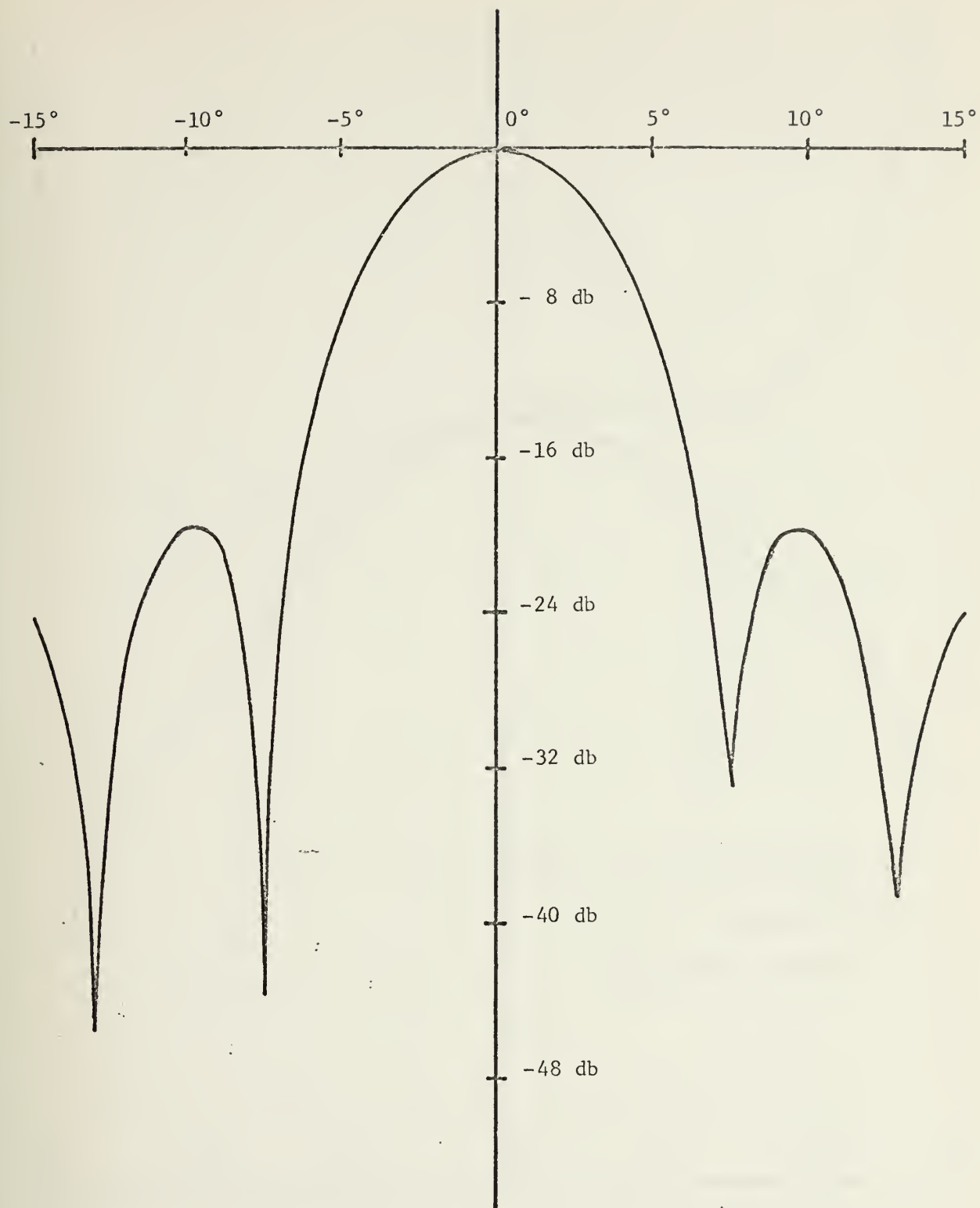


Figure 15. Luneberg Lens E-Plane Patterns for Waveguide Feed at 11 GHz.



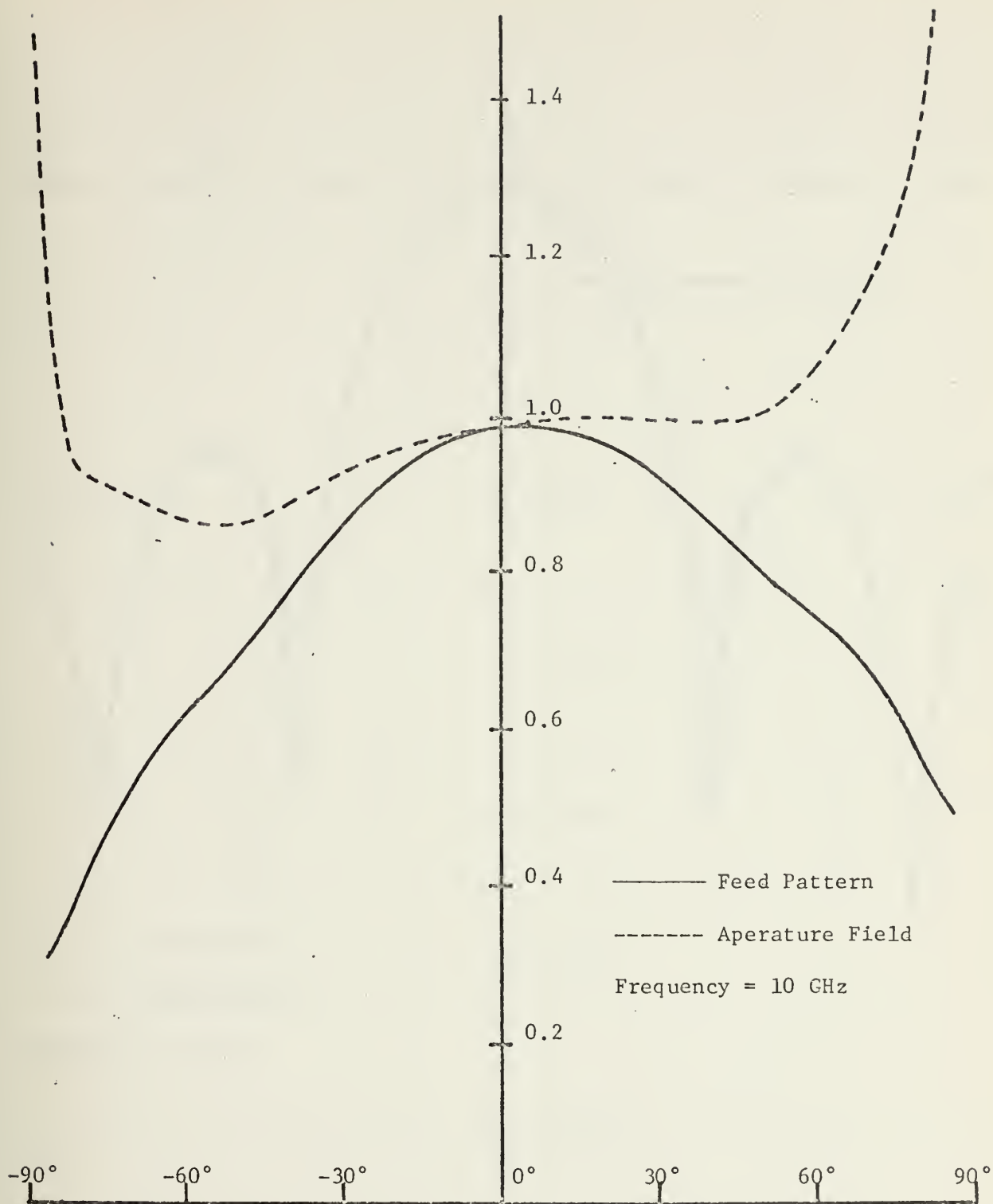


Figure 16. Yagi Array Feed Pattern and Luneberg Lens Aperture Field for Yagi Feed.



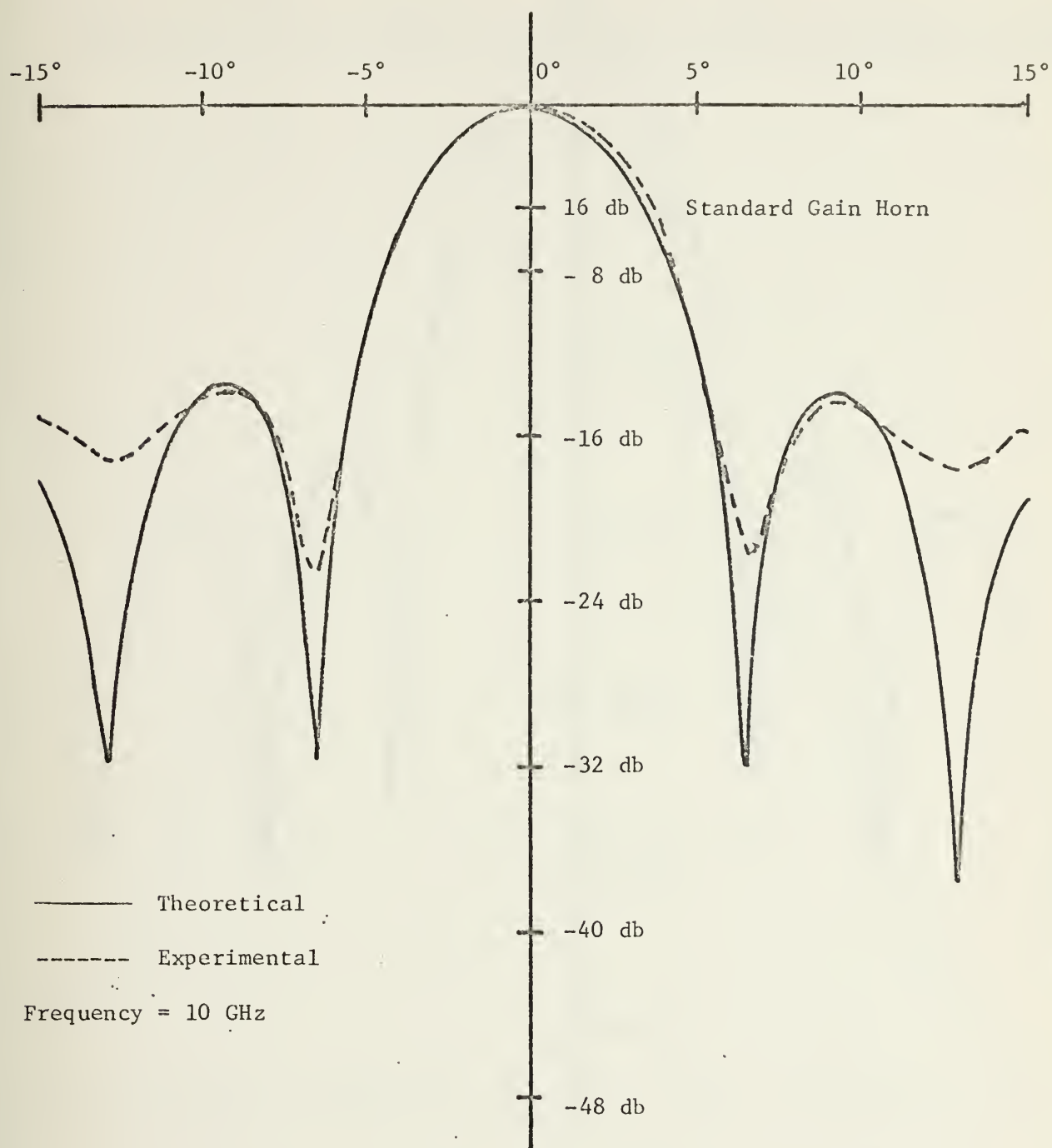


Figure 17. Luneberg Lens ( $TE_{10}$  mode) E-Plane Patterns For Yagi Feed at 10 GHz.



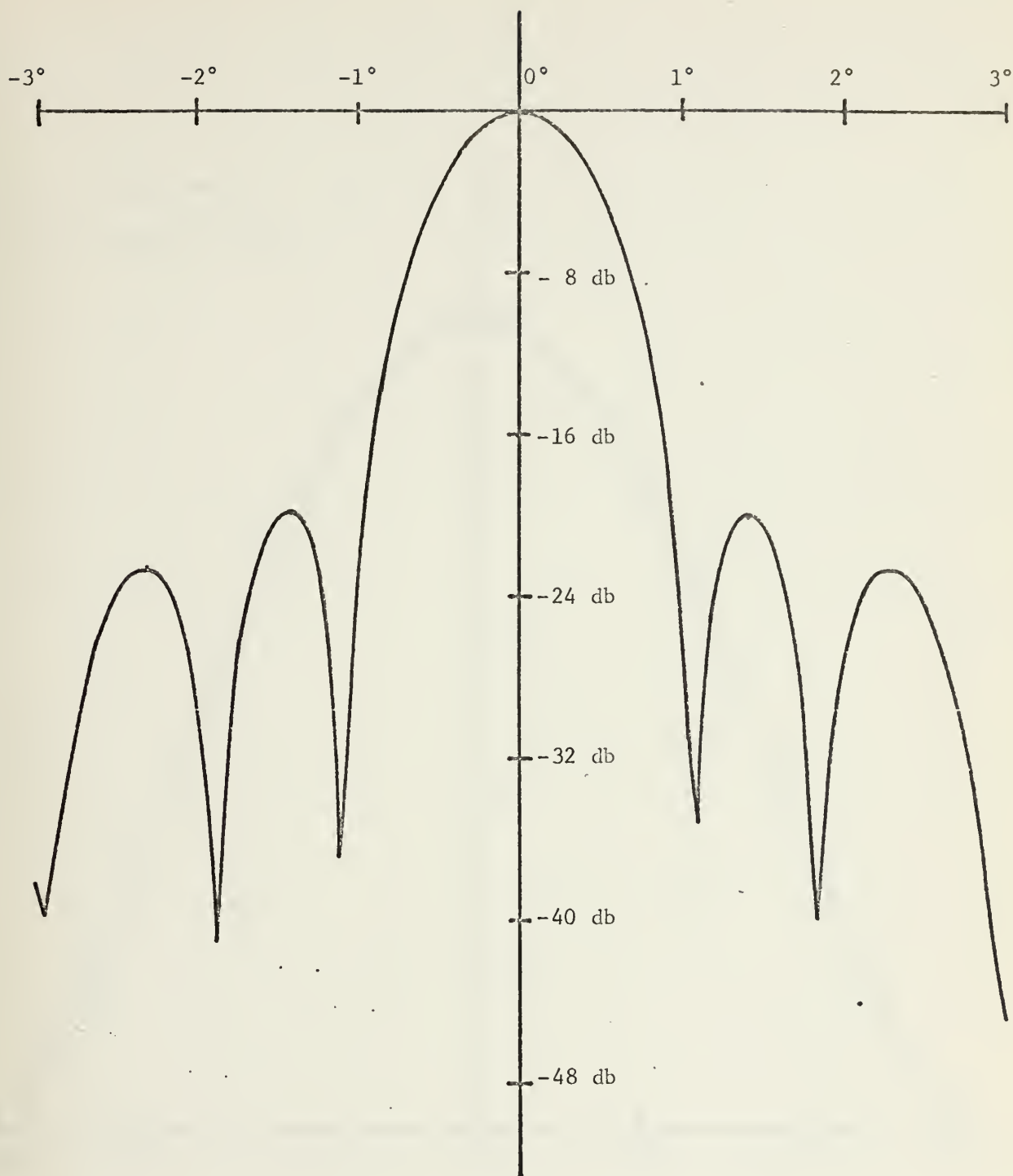


Figure 18. TEM Mode Luneberg Lens Theoretical E-Plane Radiation Patterns With Waveguide Feed at 10 GHz.



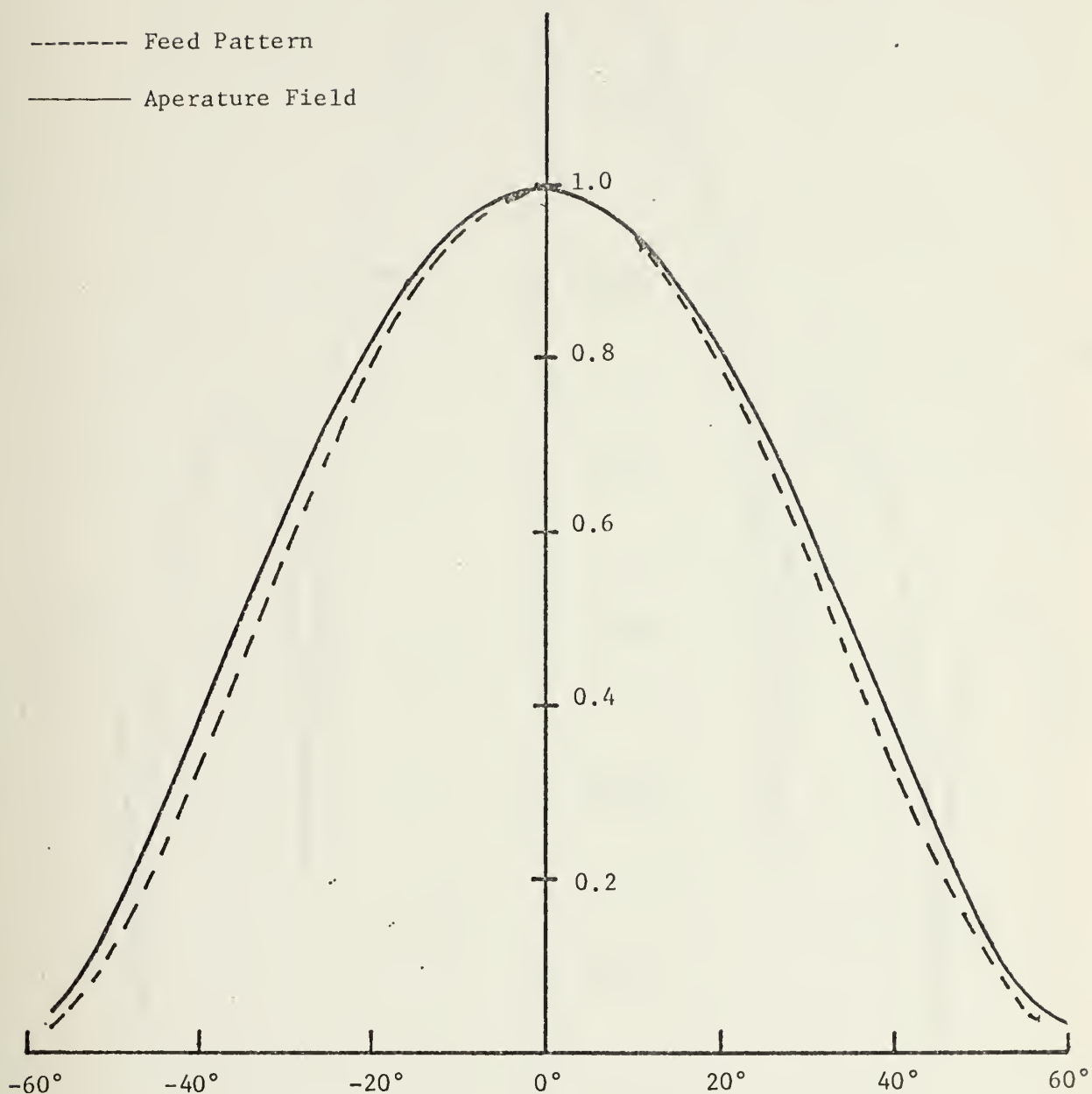


Figure 19. Dielectric Loaded Sectoral Horn Feed Patterns and Aperature Field for Sectoral Horn Feed.



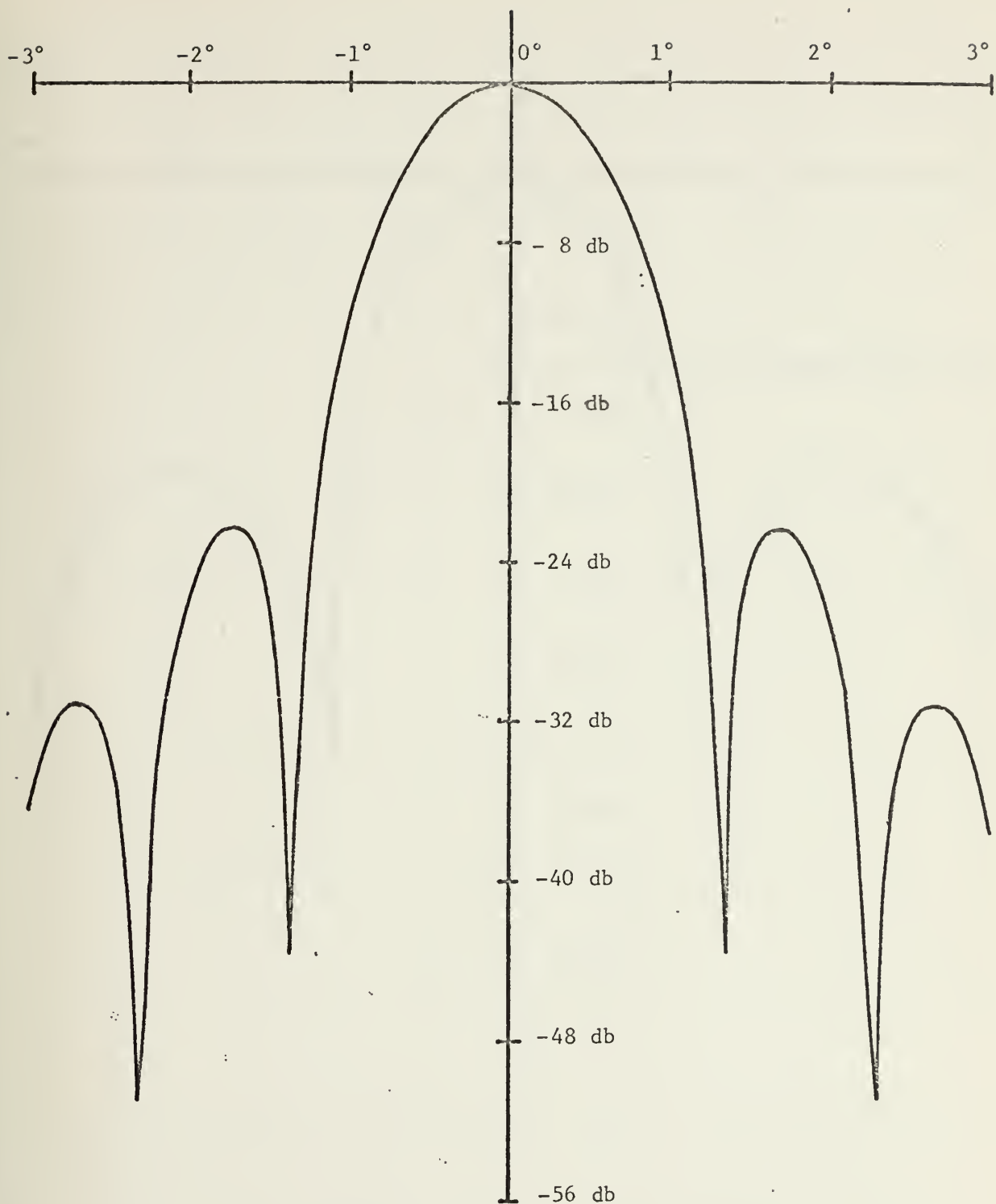


Figure 20. TEM Mode Luneberg Lens Theoretical E-Plane Radiation Patterns For Sectoral Horn Feed at 10 GHz.



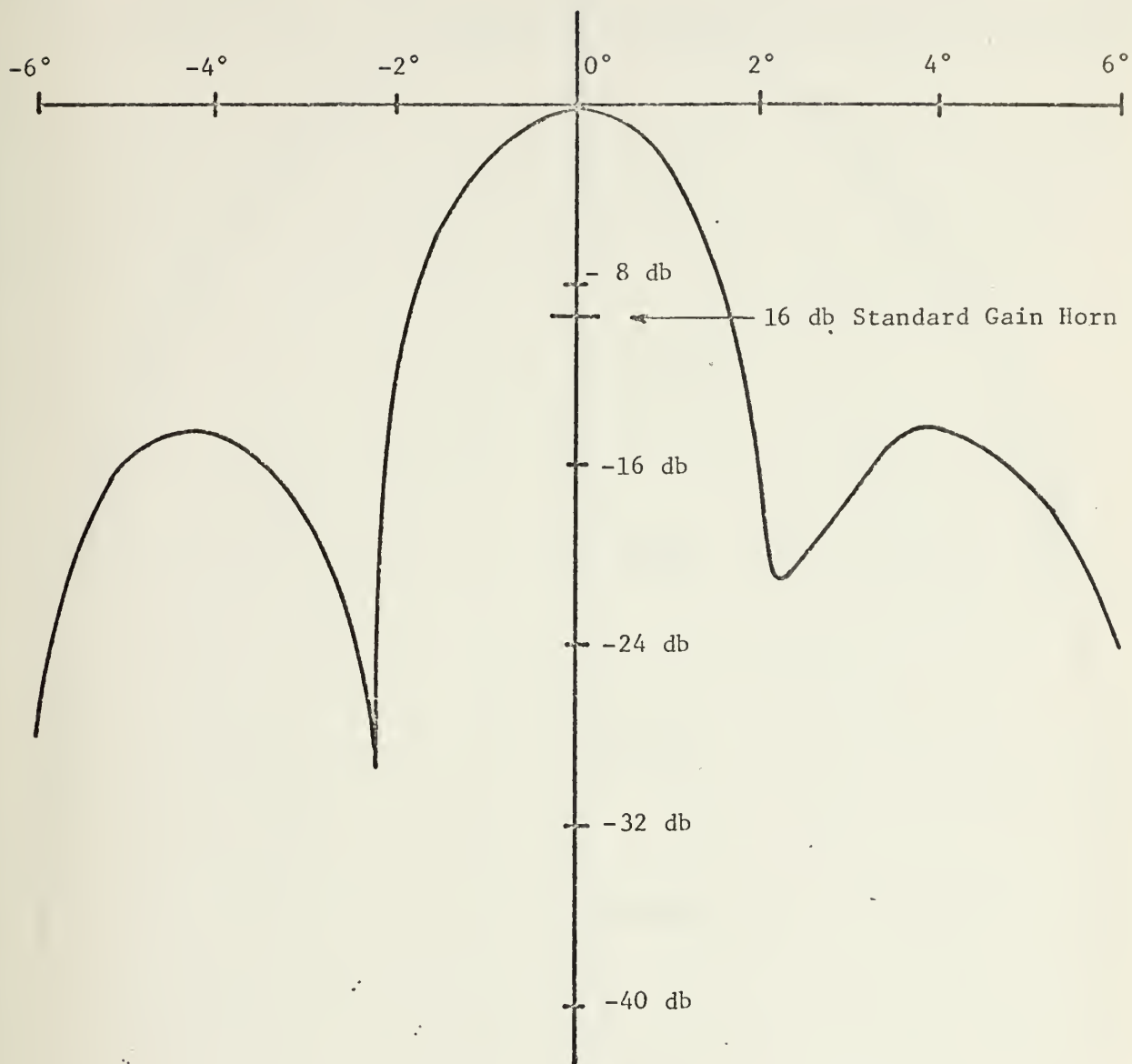


Figure 21. TEM Mode Luneberg Lens Experimental E-Plane Pattern for Sectoral Horn Feed at 10 GHz.



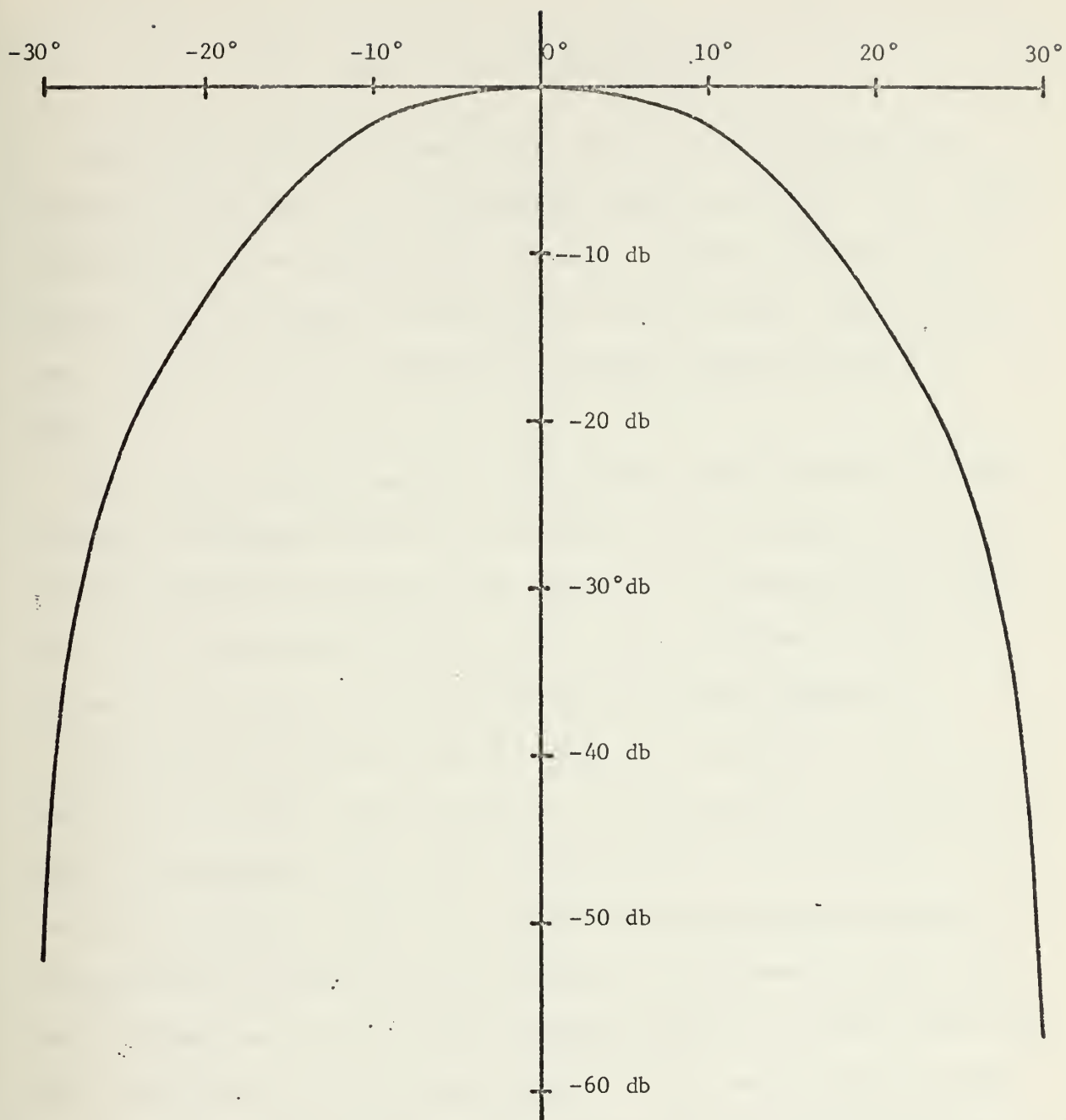


Figure 22. TEM Mode Luneberg Lens H-Plane Radiation Patterns for Sectoral Horn Feed at 10 GHz.



#### IV. CONCLUSIONS AND RECOMMENDATIONS

The results of the experimentation did not show conclusively the approach of this thesis to the problem of predicting the far field radiation patterns of the Luneberg Lens is valid. However, the results did indicate that the method is valid for the  $TE_{10}$  mode lens. There are at least two reasons for the differences, assuming that the approach is valid.

First, the far field patterns of the feed systems were used in calculating the aperture fields and far-field patterns of the lens, when in fact, the lens was not in the far field of the feeds except for the case of the Yagi array on the  $TE_{10}$  lens. This resulted in errors in the aperture fields used in calculating the far field patterns.

The results of the  $TE_{10}$  mode lens seems to confirm that this was in fact one of the major sources of error. The far field of the waveguide feed is approximately 4 cm. and it was operated at 1.7 cm from the lens for optimum side lobe levels. The differences between the theoretical and experimental patterns were an average of 0.6 degrees in first side-lobe placement and 1.5 db in first sidelobe amplitude. However, when the Yagi array feed, with a far field distance of 0.4 cm., was used at a distance of 1.7 cm from the lens, the differences in first sidelobe placement and amplitude were negligible.

The far field of the dielectric loaded sectoral horn is approximately 9.6 cm. It was operated at about 2 cm from the TEM mode lens and the results were different by about 8 db in the first sidelobe levels and 2.0 degrees in the first sidelobe placement. When the TEM mode lens was fed with the waveguide feed the first sidelobe differences were on



the order of 4.0 db in amplitude and 1.0 degrees in placement. The far field patterns of the TEM mode lens with the waveguide feed were not presented in section III due to the lack of confidence in the results.

Second, the assumption was made that the energy distribution over the x-dimension of the TEM mode lens is constant, while in fact it cannot be due to the metal plates at the top and bottom of the lens. An attempt to measure the aperture field distribution over the x-dimension of the lens failed due to the disturbance of the field caused by the dipole probe used. The x-variation of the aperture field did, however, appear to be a standing wave between the two metal plates.

It is the opinion of the author that the approach of this thesis to the far field analysis of the Luneberg Lens is valid, and that the differences between the theoretical and experimental results is almost completely due to the feed pattern information used in calculating the theoretical patterns.

In line with the above thoughts the following recommendations for future investigations are made:

A. That the near field (theoretical or experimental) of the feeds be used in the calculation of the far field radiation patterns of the Luneberg Lenses.

B. That a broad-band Yagi array, such as Yagi constructed from capacitative lumped loaded cylindrical elements, be used to feed the Luneberg Lens.

C.. That multiple Yagi arrays be used to determine the possibility of using electronically scanned Yagi array (such as in item B) to feed the Luneberg Lens in a direction finding system.



D. That the computer programs of Appendix C be modified to calculate the far field patterns of the Constant-K Lens. This would require a change of function subprograms CFCT 3 and CFCT 4 to reflect the geometric optics of the Constant-K Lens.



## APPENDIX A

### RAY PATH CALCULATIONS

#### A. DERIVATION OF RAY PATH FORMULA

The generalized Snell's Law for circular symmetry is given in Ref. 3 as

$$n(R)R \sin \theta = C_1 \quad (34)$$

when

$n(R)$  = Index of refraction

$R$  = Normalized radius

$\theta$  = Angle between ray path and outward meridian

$C_1$  = Constant

From the geometry of Figure 23,

$$\sin \theta = \frac{R d\psi}{\sqrt{(R d\psi)^2 + (dR)^2}} = \frac{R}{\sqrt{R^2 + \left(\frac{dR}{d\psi}\right)^2}} \quad (35)$$

Substituting equation (35) into (34) yields

$$C_1 = \frac{nR^2}{\sqrt{R^2 + \left(\frac{dR}{d\psi}\right)^2}} \quad \text{or} \quad d\psi = \frac{C_1 dR}{R \sqrt{n^2 R^2 - C_1^2}} \quad (36)$$

For the Luneberg Lens (normalized radius),

$$n = \sqrt{2 - R^2} \quad (37)$$

which yields

$$d\psi = \frac{C_1 dR}{R \sqrt{-R^4 + 2R^2 - C_1^2}} \quad (38)$$

or

$$\psi = C_1 \int \frac{1}{R} [-R^4 + 2R^2 - C_1^2]^{-1/2} dR. \quad (39)$$



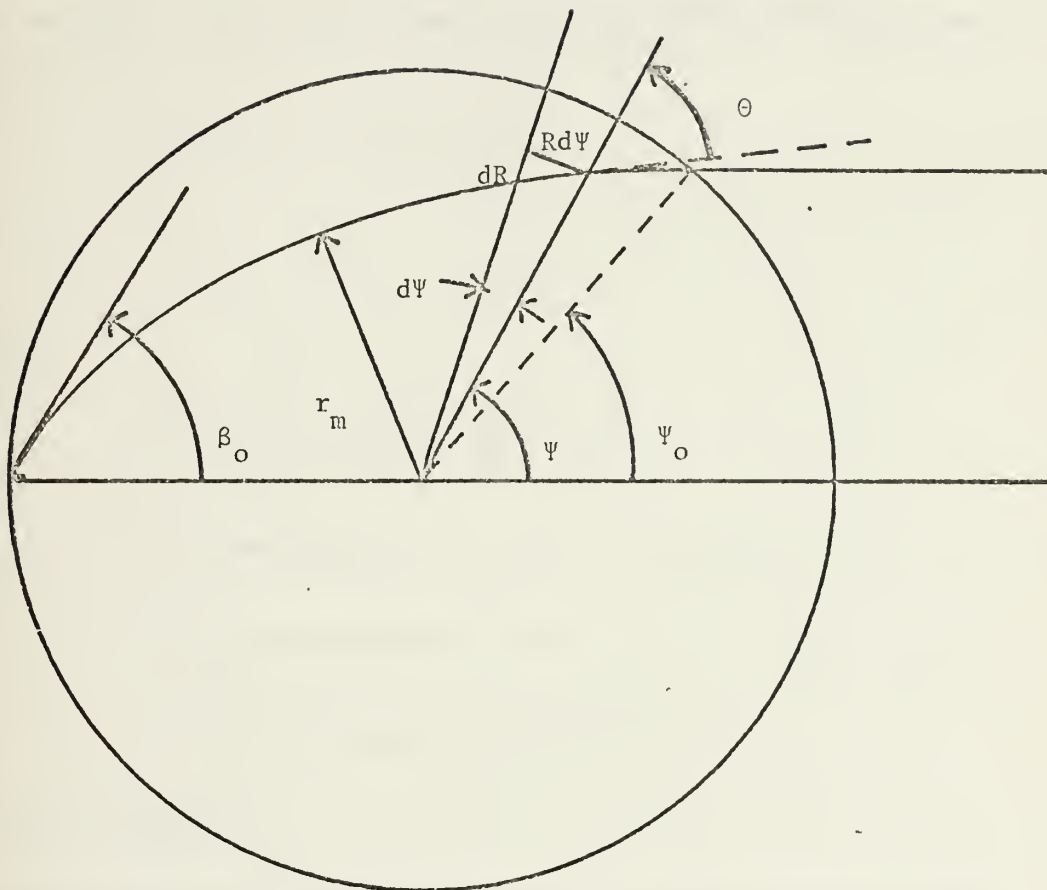


Figure 23. Geometry For Luneberg Lens Ray Path Derivations.



Integrating this equation

$$\Psi = \frac{1}{2} \sin^{-1} \sqrt{1-C_1^2} - \frac{1}{2} \sin^{-1} [(R^2-C_1^2)/(R^2\sqrt{1-C_1^2})]. \quad (40)$$

This equation gives four values of  $\Psi$  for each value of  $C_1$  and  $R$  and hence two rays. Geometrical considerations produce the following formulas:

$$\Psi_1 = \frac{\pi}{2} - \sin^{-1} \sqrt{1-C_1^2} + \Psi \quad (41)$$

and

$$\Psi_2 = \pi - \Psi, \quad (42)$$

where

$$\Psi = \int_1^R \frac{C_1}{R \sqrt{-R^4 + 2R^2 - C_1^2}} dR,$$

$$\Psi_1 \text{ corresponds to } \Psi \text{ for } \Psi_m \leq \Psi \leq \pi,$$

$$\Psi_2 \text{ corresponds to } \Psi \text{ for } \Psi_0 < \Psi < \Psi_m,$$

$$\text{and } \Psi_m \text{ is the value of } \Psi \text{ for which } R = r_m.$$

#### B. CALCULATIONS OF $r_m$ .

For each ray path the closest point of approach to the origin,  $r_m$ , occurs for  $\Theta = 90^\circ$ . Therefore, from equations (34) and (37)

$$r_m [n(r_m)] \sin 90^\circ = C_1,$$

or

$$r_m \sqrt{2-r_m^2} = C_1.$$

Squaring both sides yields

$$r_m^4 - 2r_m^2 + C_1^2 = 0$$



or, by the quadratic formula,

$$r_m = 1 \pm \sqrt{1 - C_1^2}.$$

The negative square root must be taken since the positive square root gives an  $r_m$  greater than the normalized radius. Therefore,

$$r_m = (1 - \sqrt{1 - C_1^2})^{1/2}, \quad (43)$$

which is the closest point of approach of the ray path to the center of the lens.



## APPENDIX B

### ELECTROMAGNETIC FIELD DERIVATION

#### A. DERIVATION OF ELECTRIC FIELD EQUATIONS.

The field equations for any aperture on which the electric and magnetic currents are known can be calculated utilizing the Aperture Field method and Huygen's Principle as developed in chapter 2 of Ref. 5. The electromagnetic field equations for any aperture [Ref. 5], and the geometry of Figure 24 are:

$$\vec{E} = -\frac{1}{\epsilon} \vec{\nabla} \times \vec{F} - \frac{j}{\omega\mu\epsilon} \vec{\nabla} \times \vec{\nabla} \times \vec{A} \quad (44)$$

and

$$\vec{H} = \frac{1}{\mu} \vec{\nabla} \times \vec{H} - \frac{j}{\omega\mu\epsilon} \vec{\nabla} \times \vec{\nabla} \times \vec{F}; \quad (45)$$

where

$$\vec{A} = \frac{\mu}{4\pi} \iint \frac{\vec{J}(x', \psi') e^{-jk|R_1|}}{|R_1|} dS' \quad (46)$$

$$\vec{F} = \frac{\epsilon}{4\pi} \iint \frac{\vec{K}(x', \psi') e^{-jk|R_1|}}{|R_1|} dS' \quad (47)$$

$$\vec{J}(x', \psi') = \vec{n} \times \vec{H}_a \quad (48)$$

$$\vec{K}(x', \psi') = \vec{E} \times \vec{n} \quad (49)$$

$$k = \frac{2\pi}{\lambda} \quad (50)$$

$$dS' = \rho \, dx' \, d\psi' \quad (51)$$

$$|R_1| = [R^2 + (R')^2 - 2R(x' \cos\phi \cos\theta - \rho \sin\psi' \sin\theta \sin\phi + \rho \cos\psi' \cos\theta)]^{1/2}, \quad (52)$$

$$\vec{n} = -\sin\psi' \vec{a}_y + \cos\psi' \vec{a}_z \equiv \text{unit normal to aperture.} \quad (53)$$







Equation (1) was divided into two parts:

$$\bar{E} = \bar{E}_1 + \bar{E}_2 \quad (53)$$

where

$$\bar{E}_1 = -\frac{1}{\epsilon} \bar{\nabla} \times \bar{F} \quad (54)$$

and

$$E_2 = -\frac{j}{\omega\mu\epsilon} \bar{\nabla} \times \bar{\nabla} \times \bar{A}, \quad (55)$$

and considered separately.

From equations (47), (49) and (54)

$$E_1 = -\frac{1}{\epsilon} \bar{\nabla} \times \left[ \frac{\epsilon}{4\pi} \iint \frac{\bar{K}(x', \psi')}{|R_1|} e^{-jk|R_1|} dS' \right]. \quad (56)$$

Taking all constants outside the curl equations and interchanging the order of the integration and curl operators,

$$E_1 = -\frac{1}{4\pi} \iint \bar{\nabla} \times \left[ \frac{\bar{K}(x', \psi') e^{-jk|R_1|}}{|R_1|} \right] dS'. \quad (57)$$

Using the vector identity

$$\bar{\nabla} \times \bar{K}f = \bar{\nabla}f \times \bar{K} + f(\bar{\nabla} \times \bar{K}) \quad (58)$$

where

$$f = \frac{e^{-jk|R_1|}}{|R_1|}, \quad (59)$$

equation (57) reduces to

$$\bar{E}_1 = \frac{1}{4\pi} \iint \left( jk + \frac{1}{|R_1|} \right) \left( \frac{e^{-jk|R_1|}}{|R_1|} \right) (\bar{a}_r \times \bar{K}(x', \psi')) dS', \quad (60)$$

since

$$\bar{\nabla}f = \left( \frac{-jk}{|R_1|} - \frac{1}{|R_1|^2} \right) e^{-jk|R_1|}$$

and  $\bar{\nabla} \times \bar{K} = 0$ .<sup>4</sup>

---

<sup>4</sup> $\bar{K}$  is independent of the point of observation.



From equations (46) and (55)

$$E_2 = \frac{-j}{\omega\mu\epsilon} \bar{\nabla} \times \bar{\nabla} \times \left[ \frac{-\mu}{4\pi} \iint \frac{\bar{J}(x', \psi') e^{-jk|R_1|}}{|R_1|} ds' \right].$$

Taking all constants outside the curl equations and interchanging the order of integration and the curl operators

$$E_2 = \frac{-j}{4\pi\omega\epsilon} \iint \bar{\nabla} \times \bar{\nabla} \times \left[ \frac{\bar{J}(x', \psi') e^{-jk|R_1|}}{|R_1|} \right] ds'. \quad (61)$$

Applying the vector identity of equation (58) to the integrand twice yields

$$\bar{\nabla} \times \bar{\nabla} \times \left( \frac{J(x', \psi') e^{-jk|R_1|}}{|R_1|} \right) = \left( -\frac{k^2}{|R_1|} + \frac{2jk}{|R_1|^2} + \frac{2}{|R_1|^3} \right) e^{-jk|R_1|} [\bar{a}_r \times (\bar{a}_r \times \bar{J})] \quad (62)$$

Then from equations (61) and (62)

$$E_2 = \frac{j}{4\pi\omega\epsilon} \iint \left( k^2 - \frac{2jk}{|R_1|} - \frac{2}{|R_1|^2} \right) \left( \frac{e^{-jk|R_1|}}{|R_1|} \right) [\bar{a}_r \times (\bar{a}_r \times \bar{J})] ds'. \quad (63)$$

Equations (51), (53), (60) and (63) yield the Electric Field or any cylindrical aperture field at any distance from the aperture. For the far field only, the  $1/|R_1|^2$  and  $1/|R_1|^3$  terms can be neglected leaving

$$E_1 = \frac{jk\rho}{4\pi} \iint \frac{e^{-jk|R_1|}}{|R_1|} (\bar{a}_r \times \bar{K}(x', \psi')) dx' d\psi'. \quad (64)$$

and

$$E_2 = \frac{jk^2\rho}{4\pi\omega\epsilon} \iint \frac{e^{-jk|R_1|}}{|R_1|} [\bar{a}_r \times (\bar{a}_r \times \bar{J}(x', \psi'))] dx' d\psi'. \quad (65)$$

The Luneberg Lens was designed to produce constant phase along a line perpendicular to the aperture center and therefore the aperture field



has a phase of  $k\rho(1 - \cos\Psi')$  so that:

$$\bar{E}_a = \bar{E}_{a_1} e^{jk\rho(1 - \cos\Psi')}$$

and

$$\bar{H}_a = \bar{H}_{a_1} e^{jk\rho(1 - \cos\Psi')}$$

$\bar{E}_{a_1}$  and  $\bar{H}_{a_1}$  are the E and H fields of the aperture.

$\bar{K}$  and  $\bar{J}$  can then be rewritten as

$$\bar{K} = (\bar{E}_{a_1} \times \bar{n}) e^{jk\rho(1 - \cos\Psi')} = \bar{K}_1 e^{jk\rho(1 - \cos\Psi')} \quad (66)$$

and

$$\bar{J} = (\bar{n} \times \bar{H}_{a_1}) e^{jk\rho(1 - \cos\Psi')} = \bar{J}_1 e^{jk\rho(1 - \cos\Psi')} \quad (67)$$

Equations (64) and (65) can be rewritten as

$$\bar{E}_1 = \frac{jk\rho}{4\pi} \iint \frac{e^{-jk|R_1|} e^{jk\rho(1 - \cos\Psi')}}{|R_1|} \bar{F}_1 dx' d\Psi' \quad (68)$$

and

$$\bar{E}_2 = \frac{jk^2\rho}{4\pi\omega\epsilon} \iint \left( \frac{e^{-jk|R_1|} e^{jk\rho(1 - \cos\Psi')}}{|R_1|} \right) \bar{F}_2 dx' d\Psi' \quad (69)$$

where

$$\bar{F}_1 = \bar{a}_r \times \bar{K}(x', \Psi') = \bar{a}_r \times (\bar{E}_{a_1} \times \bar{n}), \quad (70)$$

and

$$\bar{F}_2 = \bar{a}_r \times (\bar{a}_r \times \bar{J}_1(x', \Psi')) = \bar{a}_r \times [\bar{a}_r \times (\bar{n} \times \bar{H}_{a_1})] \quad (71)$$

From equation (70) and vector identity

$$\bar{A} \times (\bar{B} \times \bar{C}) = (\bar{A} \cdot \bar{C})\bar{B} - (\bar{A} \cdot \bar{B})\bar{C}, \quad (72)$$

$$\bar{F}_1 = (\bar{a}_r \cdot \bar{n})\bar{E}_{a_1} - (\bar{a}_r \cdot \bar{E}_{a_1})\bar{n},$$

or

$$\bar{F}_1 = C_7 \bar{E}_{a_1} - C_8 \bar{n}, \quad (73)$$

where

$$C_7 \equiv \bar{a}_r \cdot \bar{n},$$



and

$$C_8 = \bar{a}_r \cdot \bar{E}_{a_1}. \quad (75)$$

Assuming that the aperture field is polarized in the x-direction (i.e.

$$\bar{E}_{a_1} = E_{ax} \bar{a}_x \text{ and } \bar{H}_{a_1} = H_{ay} \bar{a}_y)$$

$$C_7 = -\sin \theta \sin \phi \sin \psi' + \cos \theta \cos \psi' \quad (76)$$

and

$$C_8 = E_{ax} \sin \theta \cos \phi. \quad (77)$$

Combining equations (73), (76) and (77) gives

$$\begin{aligned} \bar{F}_1 = & (-\sin \theta \sin \phi \sin \psi' + \cos \theta \cos \psi') E_{ax} \bar{a}_x \\ & + E_{ax} \sin \theta \cos \phi \sin \psi' \bar{a}_y \\ & - E_{ax} \sin \theta \cos \phi \cos \psi' \bar{a}_z \end{aligned} \quad (78)$$

Converting to spherical coordinates

$$\bar{F}_1 = F_{1r} \bar{a}_r + F_{1\theta} \bar{a}_\theta + F_{1\phi} \bar{a}_\phi \quad (79)$$

where

$$F_{1r} = 0, \quad (80)$$

$$F_{1\theta} = E_{ax} \cos \psi' \cos \phi, \quad (81)$$

and

$$F_{1\phi} = E_{ax} (\sin \theta \sin \psi' - \cos \theta \cos \psi' \sin \phi). \quad (82)$$

When the above equations are substituted into equation (68)

$$\bar{E} = \frac{jk_0}{4\pi} \iint \frac{e^{-jk|R_1|} e^{jk_0(1 - \cos \psi')}}{|R_1|} [F_{1r} \bar{a}_r + F_{1\theta} \bar{a}_\theta + F_{1\phi} \bar{a}_\phi] dx' d\psi' \quad (83)$$

or

$$\bar{E}_1 = E_{1r} \bar{a}_r + E_{1\theta} \bar{a}_\theta + E_{1\phi} \bar{a}_\phi \quad (84)$$

where

$$E_{1r} = 0, \quad (85)$$



$$E_{1\phi} = \frac{jk\rho}{4\pi} \iint \frac{e^{-jk|R_1|} e^{jk\rho(1 - \cos \Psi')}}{|R_1|} F_{1\phi} dx' d\Psi' \quad (86)$$

and

$$E_{1\theta} = \frac{jk\rho}{4\pi} \iint \frac{e^{-jk|R_1|} e^{jk\rho(1 - \cos \Psi')}}{|R_1|} F_{1\theta} dx' d\Psi' \quad (87)$$

Similarly, from equations (71) and (72)

$$F_2 = \bar{a}_r \times (C_9 \bar{n} - C_7 \bar{H}_a)$$

or

$$F_2 = C_9 (\bar{a}_r \times \bar{n}) - C_7 (\bar{a}_r \times \bar{H}_a), \quad (88)$$

where

$$C_9 \equiv \bar{a}_r \cdot \bar{H}_a \quad (89)$$

and

$$\begin{aligned} \bar{a}_r \times \bar{n} = & (\sin \theta \sin \phi \cos \Psi' + \cos \theta \sin \Psi') \bar{a}_x \\ & - \sin \theta \cos \phi \cos \Psi' \bar{a}_y \\ & - \sin \theta \cos \phi \sin \Psi' \bar{a}_z. \end{aligned} \quad (90)$$

Again assuming an aperture field polarized in the x-direction

$$\bar{H}_{a1} = H_{ay} \bar{a}_y, \quad (91)$$

$$\bar{a}_r \times \bar{H}_a = -H_{ay} \cos \theta \bar{a}_x + H_{ay} \sin \theta \cos \phi \bar{a}_z, \quad (92)$$

$$C_9 = H_{ay} \sin \theta \sin \phi, \quad (93)$$

and  $C_7$  is as given by equation (76). From equations (76) and (88-93)

$$\begin{aligned} \bar{F}_2 = & H_{ay} (\sin^2 \theta \sin^2 \phi \cos \Psi' + \cos^2 \theta \cos \Psi') \bar{a}_x \\ & - H_{ay} \sin^2 \theta \sin \phi \cos \phi \cos \Psi' \bar{a}_y \\ & - H_{ay} \sin \theta \cos \phi \cos \theta \cos \Psi' \bar{a}_z. \end{aligned} \quad (94)$$

Converting to spherical coordinates

$$\bar{F}_2 = F_{2r} \bar{a}_r + F_{2\theta} \bar{a}_\theta + F_{2\phi} \bar{a}_\phi \quad (95)$$



or

$$\bar{E}_2 = \frac{jk^2 \rho}{4\pi\omega\epsilon} \iint \frac{e^{-jk|R_1|} e^{jk\rho(1 - \cos \Psi')}}{|R_1|} (F_{2r} \bar{a}_r + F_{2\theta} \bar{a}_\theta + F_{2\phi} \bar{a}_\phi) dx' d\Psi' \quad (96)$$

where

$$F_{2r} = 0, \quad (97)$$

$$F_{2\theta} = H_{ay} \cos \theta \cos \Psi' \cos \phi, \quad (98)$$

and

$$F_{2\phi} = -H_{ay} \sin \phi \cos \Psi'. \quad (99)$$

When the above equations are substituted into equation (69)

$$\bar{E}_2 = \frac{jk^2 \rho}{4\pi\omega\epsilon} \iint \left[ \frac{e^{-jk|R_1|} e^{jk\rho(1 - \cos \Psi')}}{|R_1|} \right] [F_{2r} \bar{a}_r + F_{2\theta} \bar{a}_\theta + F_{2\phi} \bar{a}_\phi] dx' d\Psi' \quad (100)$$

or

$$\bar{E}_2 = E_{2r} \bar{a}_r + E_{2\theta} \bar{a}_\theta + E_{2\phi} \bar{a}_\phi; \quad (101)$$

where

$$E_{2r} = 0, \quad (102)$$

$$E_{2\theta} = \frac{jk^2 \rho}{4\pi\omega\epsilon} \iint \frac{e^{-jk|R_1|} e^{jk\rho(1 - \cos \Psi')}}{|R_1|} F_{2\theta} dx' d\Psi', \quad (103)$$

and

$$E_{2\phi} = \frac{jk^2 \rho}{4\pi\omega\epsilon} \iint \frac{e^{-jk|R_1|} e^{jk\rho(1 - \cos \Psi')}}{|R_1|} F_{2\phi} dx' d\Psi'. \quad (104)$$

From equation (53)

$$\bar{E} = \bar{E}_1 + \bar{E}_2 = E_r \bar{a}_r + E_\theta \bar{a}_\theta + E_\phi \bar{a}_\phi \quad (105)$$

where

$$E_r = E_{1r} + E_{2r} \quad (106)$$

$$E_\theta = E_{1\theta} + E_{2\theta}, \quad (107)$$

and

$$E_\phi = E_{1\phi} + E_{2\phi}. \quad (108)$$

Substituting equations (85) and (102) into (106), (87) and (103) into (107), and (86) and (104) into (108),

$$E_r = 0,$$



$$E_{\theta} = \frac{jk\rho}{4\pi} \iint \left[ \frac{e^{-jk|R_1|} e^{jk\rho(1 - \cos \psi')}}{|R_1|} \right] [E_{ax} \cos \psi' \cos \phi + \frac{k}{\omega\epsilon} H_{ay} \cos \theta \cos \psi' \cos \phi] dx' d\psi',$$

and

$$E_{\phi} = \frac{jk\rho}{4\pi} \iint \left[ \frac{e^{-jk|R_1|} e^{jk\rho(1 - \cos \psi')}}{|R_1|} \right] [E_{ax} (\sin \theta \sin \psi' - \cos \theta \cos \psi' \sin \phi) + \frac{k}{\omega\epsilon} H_{ay} \sin \phi \cos \psi'] dx' d\psi'.$$

Considering the far field relationship of E and H at the aperture of the lens

$$H_{ay} = \sqrt{\frac{\epsilon}{\mu}} \bar{E}_{ax}$$

which when substituted in the above equations yields

$$E_r = 0, \quad (109)$$

$$E_{\theta} = \frac{jk\rho}{4\pi} [\cos \phi (1 + \cos \theta)] e^{-jk\rho} \iint \frac{e^{-jk|R_1|} e^{jk\rho \cos \psi'}}{|R_1|} E_{ax} \cos \psi' dx' d\psi' \quad (110)$$

and

$$E_{\phi} = \frac{jk\rho}{4\pi} e^{jk\rho} \iint \left[ \frac{e^{-jk|R_1|} e^{jk\rho \cos \psi'}}{|R_1|} \right] [E_{ax} [\sin \theta \sin \psi' - \cos \psi' \sin \phi (1 + \cos \theta)]] dx' d\psi'. \quad (111)$$

A similar derivation for an aperture field polarized in the y-direction yields

$$E_r = 0, \quad (112)$$

$$E_{\theta} = \frac{jk\rho}{4\pi} e^{jk\rho} \iint \frac{e^{-jk|R_1|} e^{-jk\rho \cos \psi'}}{|R_1|} [E_{ay} [\cos \psi' \sin \phi (1 + \cos \theta) - \sin \theta \sin \psi']] dx' d\psi', \quad (113)$$

and

$$E_{\phi} = \frac{jk\rho}{4\pi} [\cos \phi (\cos \theta + 1)] \iint \frac{e^{-jk|R_1|} e^{-jk\rho \cos \psi'}}{|R_1|} [E_{ay} \cos \psi'] dx' d\psi', \quad (114)$$



where  $E_{ay}$  is the magnitude of the aperture field polarized in the y-direction.

The two sets of equations (109-111) and (112-114) when combined will produce the Far-Field expressions for any aperture field polarized in the x-y plane. If one is interested in the Far-Field patterns only, then comparison of equations (110) and (111) to equations (113) and (114), respectively, indicates that the normalized Far-Field patterns are identical for any aperture field polarized in the x-y plane. Therefore, in order to obtain the Far-Field patterns, only one set of the equations need be considered.



# APPENDIX C

## LUNEBERG LENS RAY PATHS

```

C      IMPLICIT REAL*8(A-H,R,P)
C      VARIABLES USED IN THE PROGRAM ARE:
C          C1-RAY PATH CONSTANT.
C          RMIN-CLOSEST POINT OF APPROACH OF RAY PATHS TO
C          LENS CENTER.
C          YRAY- Y-COMPONENT OF A RAY PATH POINT.
C          XRAY- X-COMPONENT OF A RAY PATH POINT.
C          R- NORMALIZED LENS RADIUS.
C      REAL LABEL /' '/
C      REAL*8 TITLE(12)
C      READ TITLE TO BE TYPED AT BOTTOM OF GRAPH
C      READ(5,100) TITLE
100    FORMAT(6A8)
C      FCT5 IS A FUNCTION WHICH WHEN INTEGRATED DESCRIBES
C      THE RAY PATHS THROUGH THE NORMALIZED LUNEBERG LENS.
C      EXTERNAL FCT5
C      DIMENSION XRAY(1100),YRAY(1100),AUX(25)
C      COMMON C1
C      INITILIZE C1 FOR THE 1ST RAY.
C      C1=0.900
C      PI=3.141592650
C      ENTER LOOP TO OBTAIN DIFFERENT RAYS
C      DO 1 I=1,9
C      CALCULATE RMIN
C      RMIN=DSQRT(1.000-DSQRT(1.000-C1**2))
C      R=1.000
C      ASTP=0.002500
C      NUM=((R-RMIN)/ASTP)+1
C      RHC=DARSIN(C1)
C      N=2*NUM
C      K=N
C      M=1
C      PH=PI/2.000-DARSIN(DSQRT(1.000-C1**2))
C      RR=R
C      X1=R*DCCS(RHO)
3      IF(1.0.LE.X1) GO TO 2
C      CALCULATION OF RAY EXTENDING IN FRONT OF LENS.
C      K=K+1
C      X1=X1+0.005
C      XRAY(K)=X1
C      YRAY(K)=C1
C      GO TO 3
C      CALL INTEGRATING SUBROUTINE TO SOLVE INTEGRAL EQ
2      CALL DQATR(RR,1.00,0.0000001,15,FCT5,DAL,IER7,AUX)
C      CALCULATE X AND Y VALUES TO BE USED IN PLOTTING RAYS
C      PHI=PH+DAL
C      PH2=PI-DAL
C      XRAY(N)=RR*DCCS(PHI)
C      YRAY(N)=RR*DSIN(PHI)
C      XRAY(M)=RR*DCCS(PH2)
C      YRAY(M)=RR*DSIN(PH2)
C      IF(N-M.LE.1) GO TO 4
C      N=N-1
C      M=M+1
C      RR=RR-ASTP
C      GO TO 2
C      ENTER INTO CONTROL FOR PLOTTING RAYS
4      IF(1.GT.1)GO TO 5
6      MOD=1
C      GO TO 7
5      MOD=2
7      CALL DRAW(K,XRAY,YRAY,MOD,0,LABEL,TITLE,0,0,4,4,2,2,8,
18,0,LAST)
C      IF(MOD.NE.1)GO TO 300
C      MOD=2

```



```

      GO TO 400
300   IF(I.GE.9) GO TO 350
      GO TO 400
350   MCD=3
400   DO 500J=1,K
500   YRAY(J)=-YRAY(J)
      CALL DRAW(K,XRAY,YRAY,MOD,0,LABEL,TITLE,0,0,4,4,2,2,8,
18,0, LAST)
      C1=C1-0.1DO
1    CONTINUE
      STOP
      END

```

```

C    FUNCTION FCT5(RAN)
C    FCT5 IS A CUNCTION WHICH WHEN INTEGRATED DESCRIBES
C    THE RAY PATHS THROUGH THE LUNEBERG LENS.
      IMPLICIT REAL *8(A-H,R,P)
      COMMON C1
      FCT5=C1/(RAN*DSQRT(-(RAN**4)+2.0DO*(RAN**2)-(C1**2)))
      RETURN
      END

```



FEED PATTERN FITTING  
AND  
APERATURE FIELD CALCULATIONS

```

C      THIS PROGRAM WAS DESIGNED TO FIT A LEAST SQUARE
C      POLYNOMINIAL TO A NUMBER OF POINTS FOR A MEASURED
C      FEED PATTERN AND THEN PLOT THE FEED FUNCTION BY USING
C      THREE TIMES AS MANY POINTS (K2) IN ORDER TO DETECT ANY
C      EXCURSION THAT THE POLYNOMINIAL FIT MAY HAVE TAKEN
C      BETWEEN TWO ADJACIENT POINTS .
      IMPLICIT REAL*8(D)
      DIMENSION DTHETA(100),DMAG(100),DA(20),DWI(80),DY(80),
      1DELY(80),A(20),DSA(20),THETA(200),EMAG(200),DTHE(100)
      2,EMA(200)
      REAL*8 DTITL(10)/10* ' ' /
      REAL LABEL/' ' /
      REAL*8 TITLE(12)
C      READ GRAPH TITLE
      READ(5,100) TITLE
      100  FORMAT(6A8)
C      M IS THE DEGREE OF POLYNOMINIAL TO BE FITTED
C      N IS THE NUMBER OF POINTS IN THE CURVE TO BE FITTED.
      READ(5,200)M,N
      200  FORMAT(I3/I2)
C      READ IN DATA POINTS-DTHETA IS THE ABSISSIA VALUE AND
C      DMAG IS THE SQUARE OF THE ORDINATE VALUE-SQUARE LAW
C      DETECTOR WAS USED TO OBTAIN DATA.
      READ(5,400) (DTHETA(I),DMAG(I),I=1,N)
      60  DO 60 J=1,N
      400  DMAG(J)=DSQRT(DMAG(J))
      FCFORMAT(F10.7,F12.6)
      DO 50 I=1,N
      50  DTHE(I)=DTHETA(I)*(3.14159265D0/180.D0)
      DO 5 I=1,N
      5  DWI(I)=1.0D0
C      LSCPL2 WILL CALCULATE THE LEASE SQUARE POLUNOMINIAL
C      CCEFFICIENTS.
      CALL LSCPL2(N,M,DTHE , DMAG,DWI,DY,DELY,DA,DSA,DTITL)
      L=1+IABS(M)
      DO 6 I=1,L
      6  A(I)=DA(I)
      WRITE(6,300) (I,A(I),I=1,L)
      300  FORMAT(' ',A(' ',I4,' ')=' ',F18.6)
      THET=DTHE(1)
      K2=3*N
C      CALCULATE SIZE OF STEPS TO BE USED IN PLCTTING CURVE.
      STEP=(DTHE(N)-DTHE(1))/K2
      WRITE(6,302)
      302  FORMAT(' ',4X,'THET',12X,'EMAG')
      DO 3 K=1,K2
      THETA(K)=THET
      EM=A(1)
      DO 4 J=2,L
      4  EM=EM+A(J)*THETA(K)**(J-1)
      EMAG(K)=EM
      WRITE(6,301) THET,EMAG(K)
      301  FORMAT(' ',F10.5,5X,F10.7)
      THET=THET+STEP
      3  CCNTINUE
C      CALCULATE THE APERATURE FIELD STRENGTH
      DO 7 K=1,K2
      EMA(K) =EMAG(K)*SQRT(1.0/COS(THETA(K)))
      WRITE(6,301)THETA(K),EMA(K)
      7  CCNTINUE
      DO 8 K=1,K2
      THETA(K)=THETA(K)*180.0/3.1415
      8  CCNTINUE
      CALL DRAW(K2 ,THETA,EMAG,1,0,LABEL,TITLE,20.0,0,0,3,2,
      12,6,7,1,LAST)
      CALL DRAW(K2 ,THETA,EMA ,3,0,LABEL,TITLE,20.0,0,0,3,2,
      12,6,7,1,LAST)
      STCP

```



END



# PHE-COMPONENT LUNEBERG LENS PATTERNS

```

C      THIS PROGRAM WAS DESIGNED TO CALCULATE PHE-COMPONENT
C      OF THE RADIATION PATTERNS OF THE CYLINDRICAL LUNEBERG
C      LENS WITH BEAM CENTERED AT 0-DEGREES, FOR A VERTICALLY
C      POLARIZED FEED. THIS PATTERN IS IDENTICAL FOR ANY FEED
C      POLARIZATION IN THE X-Y PLANE
      IMPLICIT COMPLEX(C)
      COMPLEX CJ/(0.0,1.0)/
      M=0
C      STEP IS THE STEP-SIZE IN DEGREES BETWEEN POINTS WHERE
C      THE FIELD STRENGTH IS CALCULATED.
C      THETA1 IS THE INITIAL ANGLE IN DEGREES FOR WHICH THE
C      FIELD STRENGTH IS CALCULATED.
C      THETA2 IS THE FINAL ANGLE IN DEGREES FOR WHICH THE
C      FIELD STRENGTH IS CALCULATED.
C      ANGPD IS THE ANGLE IN DEGREES THAT CONTROLS THE PLANE
C      IN WHICH THE LENS PATTERNS ARE CALCULATED, IF 90
C      DEGREES THE E-PLANE PATTERNS ARE CALCULATED, IF
C      0-DEGREES THEN THE VERTICAL BEAM PATTERN IS CALCULAT-
C      ED.
      READ(5,2) STEP, THETA1, THETA2, ANGPD
      2      FORMAT(F12.3/F12.3/F12.3/F12.3)
      PIE=3.1415926535
      ANGP=ANGPD*(PIE/180.0)
C      CALCULATE NUMBER OF STEPS, NUM, WHICH IS ALSO THE
C      NUMBER OF POINTS TO BE PLOTTED BY SUBROUTINE DRAW.
      NUM=(THETA2-THETA1)/STEP +1
C      MO IS THE INTEGER THAT CONTROLS THE NUMBER OF PLOTS
C      TO BE PLOTTED BY DRAW IN SUBROUTINE EPHEE.
C      RADIUS IS THE RADIUS OF THE LUNEBERG LENS.
C      FREQ IS THE FREQUENCY FOR WHICH THE PATTERNS ARE
C      CALCULATED.
C      THICK IS THE HEIGHT OR X-DIMENSION OF THE LENS.
      12      READ(5,4) MO, RADIUS, FREQ, THICK
      4      FORMAT(I1/F12.3/F12.3/F12.3)
      IF(MO .EQ.0) GO TO 14
      M=M+1
      14      WRITE(6,5) THETA1, THETA2, STEP, RADIUS, FREQ, NUM, MO,
      1      THICK, ANGPD
      5      FORMAT(' ', THETA1=' ', F11.6, '/', ' ', THETA2=' ', F11.6, '/', '
      1      ', 'STEP=' ', F11.6, '/', ' ', RADIUS=' ', F11.6, '/', ' ',
      2      'FREQUENCY=' ', F11.6, '/', ' ', NUM=' ', I6, '/', ' ', 'MC' ' ', I6, /
      3      ', THICK=' ', F11.6, '/', ' ', 'PHE=' ', F11.6)
      R=200.0
C      AK IS THE PROPAGATION CONSTANT.
      AK=20.0*PIE*FREQ/3.0
      CJKR=(CJ*AK*RADIUS/(4.0*PIE*R))*CEXP(CJ*AK*(RADIUS-R))
C      CJKRN IS THE NORMALIZED COEFFICIENTS
      CJKRN=CJKR/CABS(CJKR)
      100      WRITE(6,100) CJKRN
      100      FORMAT(' ', CJKRN=' ', F11.9, 2X, 'J', F11.9)
      CALL EPHEE(AK, THICK, ANGP, THETA1, STEP, NUM, CJKRN, RADIUS
      1, MC, FREQ, M)
C      EPHEE WILL CALCULATE AND PLOT THE PHE-COMPONENTS
C      OF THE E-FIELD OF THE LUNEBERG LENS
      IF(MO .EQ.0) GO TO 13
      13      STOP
      END

      SUBROUTINE EPHEE (AK1, TH1, ANGP1, ANGT1, STE, NUM, CJKRN,
      1, RA, MOD, FRE, M1)
C      THIS SUBROUTINE WAS WRITTEN TO CALCULATE AND PLOT
C      THE PHE-COMPONENT OF THE ELECTRIC FIELD OF THE LUNE-
C      BERG LENS FOR ANY FEED FUNCTION OR ANY MEASURED FEED
C      DISTRIBUTION THAT CAN BE APPROXIMATED BY A CURVE
C      FITTING TECHNIQUE.
      IMPLICIT COMPLEX(C)
C      THE NEXT FOUR STATEMENTS CONTROL THE LABELING AND

```



```

C      TITLING OF THE GRAPHS PLOTTED BY SUBROUTINE DRAW.
      REAL LABEL /' ' /
      REAL *8 TITLE(12)
      READ(5,100) TITLE
100    FORMAT(6A8)
      COMPLEX CJ/(0.0,1.0)/
      EXTERNAL CFCT1,CFCT3
C      CFCT1 IS A FUNCTION DESCRIBING THE FAR FIELD OF THE
C      LUNEBERG LENS IN TERMS OF THE APPERATURE FIELD
C      DISTRIBUTION IN THE X-DIRECTION.
C      CFCT3 IS A FUNCTION DESCRIBING THE FAR FIELD OF THE
C      LUNEBERG LENS IN TERMS OF THE APPERATURE FIELD
C      DISTRIBUTION AS A FUNCTION OF THE
C      ANGULAR DISPLACEMENT FROM BEAM CENTER.
      DIMENSION THETA(400),CEPHE(400),EPHEM(400),RADI(5),
1      FREQ(5)
      COMMON/ALIM/ALIM1,ALIM2,THIC
      COMMON AK,ANGP,THETR,RAD,L3,L1
      THIC=THI
      RAD=RA
      RADI(M1)=RA
      FREQ(M1)=FRE
      AK=AK1
      ANGP=ANGP1
      PIE=3.14159265358
      THET=ANGT1
      TH2=-THI/2.0
      TH3=THI/2.0
      ANCRM=0.0
C      ANORM IS A VARIABLE USED TO NORMALIZE THE ELECTRIC
C      FIELD STRENGTH.
C      ENTER LOOP TO CALCULATE THE E-FIELD FOR NUM-POINTS
      DO 1 I=1,NUM
      L1=I
      L3=I
      THETR=THET*(PIE/180.0)
      CALL CWEDF(CFCT1,TH2,TH3,15,CEPH1)
      L1=2
900    XL=ALIM1
      XU=ALIM2
      CALL CWEDF(CFCT3,XL,XU,375,CEPH3)
      IF(L3.NE.-1) GO TO 1000
      L3=2
      GO TO 900
1000   CEPH=CEPH1*CEPH3
      IF(ANORM.GE.CABS(CEPH)) GO TO 2
      ANORM=CABS(CEPH)
      THETA(1)=THET
      CEPHE(1)=CEPH
      THET=THET+STE
      CONTINUE
C      ENTER LOOP TO NORMALIZE AND CALCULATE THE MAGNITUDE
C      OF THE E-FIELD (EPHEM).
      DO 3 J=1,NUM
      CEPHE(J)=CEPHE(J)/ANORM
      EPHEM(J)=CABS(CEPHE(J))
      CONTINUE
      WRITE(6,84)RADI(M1),FREQ(M1)
84     FORMAT('1','PHE-COMPONENT OF THE E-FIELD FOR LENS',
1      'RADIUS OF',F8.4,2X,'METERS AT',F8.3,2X,'GFZ',/' ',6X
2      ',THETA',12X,'FIELD STRENGTH',10X,'COMPLEX FIELD ',
3      'STRENGTH')
      J=0
      DO 23 I=1,NUM
      WRITE (6,85)THETA(I),EPHEM(I),CEPHE(I)
85     FORMAT(' ','F11.3,8X,F14.6,12X,F10.6,F10.6)
      J=J+1
      IF(J.LT.72)GO TO 23
      WRITE(6,84)RAD,FRE
      J=0
23    CONTINUE
C      ENTER LOOP TO CALCULATE THE FIELD MAGNITUDES IN DECI-

```



```

C      BELS.
      DO 20 I=1, NUM
      EPHEM(I)=20.0*ALOG10(EPHEM(I))
20     CCNTINUE
      CALL DRAW(NUM, THETA, EPHEM, MOD, 0, LABEL, TITLE, 0, 8.0, 7, 3,
90     12, 2, 6, 8, 1, LAST)
      RETURN
      END

```

```

      SUBROUTINE CWEDF (CF, XL, XU, NX, CANS)
      CWEDF WAS OBTAINED FROM LCDR. E.G. NEELY .
      CWEDF IS A SUBROUTINE WHICH WILL NUMERICALLY
      INTEGRATE A USER SUPPLIED FUNCTION BETWEEN SPECIFIED
      LIMITS. (SINGLE PRECISION)
      CF      - NAME OF FUNCTION SUBPROGRAM.  MUST BE
      LISTED IN AN EXTERNAL STATEMENT.
      XL      - LOWER LIMIT OF INTEGRATION
      XU      - UPPER LIMIT OF INTEGRATION
      NX      - APPROXIMATE NUMBER OF NODES AT WHICH TO
      EVALUATE THE FUNCTION.
      CANS    - RESULT OF INTEGRATION

```

```

      IMPLICIT COMPLEX*8 (C)
      REAL*8 DXDX, XX
      REAL*4 CW(6)/82., 216., 27., 272., 27., 216./
      COMMON AK, ANGP, THETR, RAD, L3, L1
      IF(NX.LE.0) GO TO 900
      N=((NX+4)/6)*6+1
      DX=(XU-XL)/FLOAT(N-1)
      DXDX=DBLE(DX)
      NWIX=N/6
      X=XL
      CANS=-CF(X)*41.0
      IF(L3.EQ.-1) GO TO 1000
      IF(L1.EQ.1) GO TO 500
      IF(L3.NE.1) GO TO 500
      L2=2
500     DO 800 MX=1, NWIX
      DC 700 KX=1, 6
      CANS=CANS+CW(KX)*CF(X)
      XX=DBLE(X)
      X=SNGL(XX+DXDX)
700     CONTINUE
800     CONTINUE
      CANS=(CANS+41.0*CF(X))*DX/140.0
      RETURN
900     WRITE(6, 901) N
901     FORMAT('OERROR IN CALLING PARAMETER ***** N = ',
115, ' *****'//)
1000    RETURN
      END

```

```

      FUNCTION CFCT1(X)
      CFCT1 IS A FUNCTION WHICH DESCRIBES THE FAR-FIELD
      VARIATIONS OF THE E-FIELD AS A FUNCTION OF THE LUNE-
      BERG LENS HEIGHT.
      IMPLICIT COMPLEX(C)
      COMPLEX CJ/(0.0, 1.0)/
      COMMON AK, ANGP, THETR, RAD, L3, L1
      COMMON/ALIM/ALIM1, ALIM2, THIC
      CEX=CJ*AK*SIN(THETR)*COS(ANGP)*X
      CFCT1=CEX*EXP(CEX)*COS(3.14159*X/THIC)
      RETURN
      END

```



```

C      FUNCTION CFCT3(ANG)
C      CFCT3 IS A FUNCTION WHICH DESCRIBES THE FAR FIELD
C      VARIATIONS OF THE E-FIELD AS A FUNCTION OF ANG
C      (THE ANGLE FROM BEAM CENTER). TO DO THIS LSCPL2 IS
C      UTILIZED TO FIT A CURVE TO THE MEASURED FEED FUNCTION
C      AND COMBINES THIS WITH THE OTHER ANGULAR VARIATIONS
C      OF THE FAR-FIELD EQUATIONS.
C      IMPLICIT REAL*8(D)
C      IMPLICIT COMPLEX (C)
C      COMPLEX CJ/(0.0,1.0)/
C      DIMENSION DTHETA(100),DMAG(100),DA(20),DWI(80),DY(80),
1      DELY(80),A(20),DSA(20),THETA(100),EMAG(100),DTHE(100)
C      REAL*8 DTITL(10)/10*'/
C      COMMON AK,ANGP,THETR,RAD,L3,L1
C      COMMON/ALIM/ALIM1,ALIM2,THIC
C      L3 WILL BE EQUAL TO 1 ON THE FIRST CALL OF CFCT3
C      AND WILL PROCEED THROUGH THE NEXT STEPS DOWN TO 600
C      IN ORDER TO CALCULATE THE POLYNOMIAL COEF. THAT
C      DESCRIBE THE FEED FUNCTION.
C      IF L3 IS NOT 1, THEN THE POLYNOMIAL COEF. HAVE BEEN
C      CALCULATED BY A PREVIOUS PASS.
C      IF(L3.NE.1) GO TO 600
C      READ(5,200) M,N
200      FORMAT(I3/I2)
C      READ(5,400) (DTHETA(I),DMAG(I),I=1,N)
400      FORMAT(F10.7,F12.6)
C      DO 60 J=1,N
60      DMAG(J)=DSQRT(DMAG(J))
C      DO 50 I=1,N
50      DTHE(I)=DTHETA(I)*(3.14159265D0/180.D0)
C      ALIM1=DTHE(1)
C      ALIM2=DTHE(N)
C      DO 5 I=1,N
5      DWI(I)=1.0D0
C      CALL LSCPL2(N,M,DTHE , DMAG,DWI,CY,DELY,DA,DSA,DTITL)
C      L=1+IABS(M)
C      DO 6 I=1,L
6      A(I)=DA(I)
C      THETA(I)=DTHETA(I)
300      WRITE(6,300) (I,A(I),I=1,L)
C      FORMAT(' ','A(',I4,')=' ,F18.6)
C      L3=-1
C      RETURN
600      EM=A(1)
C      DO 4 J=2,L
4      EM=EM+A(J)*ANG**(J-1)
C      EAL IS A FUNCTION WHICH DESCRIBES THE FEED VARIATIONS
C      OVER THE PLANE OF THE LENS.
C      EAL=EM
C      CER=CJ*AK*RAD*(COS(ANG)*(COS(THETR)-1.0)-SIN(ANG)*
1      SIN(THETR)*SIN(ANGP))
C      THE SQRT(1.0/COS(ANG)) TERM IS THE ONLY PART OF THIS
C      EQUATION ASSOCIATED WITH THE LENS FUNCTION.
C      THE REMAINDER IS FROM THE APPLICATION OF THE APERTURE
C      FIELD METHOD TO THE SEMI-CIRCULAR APERTURE. TO MOD-
C      IFY THIS PROGRAM TO PREDICT THE CONSTANT-K LENS FAR
C      FIELD PATTERNS CHANGE THIS FUNCTION. THE CORRECT PHASE
C      TERMS ARE ALREADY INCLUDED.
C      CFCT3=CEXP(CER)*(SIN(THETR)*SIN(ANG)-COS(ANG)*
1      SIN(ANGP)*(COS(THETR)+1.0))*SQRT(1.0/COS(ANG))*EAL
C      RETURN
C      END

```



# THETA-COMPONENT LUNEBERG LENS PATTERNS

```

C      THIS PROGRAM WAS DESIGNED TO CALCULATE THE THETA COM-
C      PONENT OF THE CYLINDRICAL LUNEBERG LENS RADIATION PAT-
C      TERNS WITH BEAM CENTERED AT 0-DEGREES, FOR ANY FEED
C      POLARIZED IN THE X-Y PLANE.
      IMPLICIT COMPLEX(C)
      COMPLEX CJ/(0.0,1.0)/
      M=0
C      STEP IS THE STEP-SIZE IN DEGREES BETWEEN POINTS WHERE
C      THE FIELD STRENGTH IS CALCULATED.
C      THETA1 IS THE INITIAL ANGLE IN DEGREES FOR WHICH THE
C      FIELD STRENGTH IS CALCULATED.
C      THETA F IS THE FINAL ANGLE IN DEGREES FOR WHICH THE
C      FIELD STRENGTH IS CALCULATED.
C      ANGP D IS THE ANGLE IN DEGREES THAT CONTROLS THE PLANE
C      IN WHICH THE LENS PATTERNS ARE CALCULATED, IF 90
C      DEGREES THE E-PLANE PATTERNS ARE CALCULATED, IF
C      0-DEGREES THEN THE VERTICAL BEAM PATTERN IS CALCULAT-
C      ED.
      READ(5,2) STEP, THETA1, THETA F, ANGP D
      FORMAT(F12.3/F12.3, F12.3/F12.3)
      PIE=3.1415926535897
      ANGP=ANGP D*(PIE/180.0)
C      CALCULATE NUMBER OF STEPS REQUIRED WHICH IS THE SAME
C      AS THE NUMBER OF POINTS TO BE PLOTTED BY DRAW
      NUM=(THETA F-THETA1)/STEP +1
C      MO IS THE INTEGER THAT CONTROLS THE NUMBER OF PLOTS
C      TO BE PLOTTED BY DRAW IN SUBROUTINE ETHETA
C      RADIUS IS THE RADIUS OF THE LUNEBERG LENS.
C      FREQ IS THE FREQUENCY FOR WHICH THE PATTERNS ARE
C      CALCULATED.
C      THICK IS THE HEIGHT OF THE LENS.
12      READ(5,4) MO , RADIUS, FREQ, THICK
      FORMAT(I1/F12.3/F12.3/F12.3)
      IF(MO .EQ.0) GO TO 14
      M=M+1
14      WRITE(6,5) THETA1, THETA F, STEP, RADIUS, FREQ, NUM, MO,
1      THICK, ANGP D
      FORMAT(' ', THETA1=' ', F11.3, /, ' ', THETA F=' ', F11.3, /,
1      ' ', STEP=' ', F11.6, /, ' ', RADIUS=' ', F11.6, /, ' ',
2      ' FREQUENCY=' ', F11.6, /, ' ', NUM=' ', I6, /, ' ', MC=' ', I6
3      /, ' ', THICK=' ', F11.6, /, ' ', PFE=' ', F11.6)
      R=200.0
C      AK IS THE PROPAGATION CONSTANT.
      AK=20.0*PIE*FREQ/3.0
      CJKR=(CJ*AK*RADIUS/(4.0*PIE*R))*CEXP(CJ*AK*(RADIUS-R))
      CJKRN=CJKR/CABS(CJKR)
      WRITE(6,100) CJKRN
100      FORMAT(' ', CJKRN=' ', F11.9, 2X, 'J', F11.9)
      CALL ETHETA(AK, THICK, ANGP, THETA1, STEP, NUM, CJKRN, RADIUS
1      MC, FREQ, M)
C      ETHETA WILL CALCULATE AND PLOT THE THETA COMPONENTS
C      -FIELD PATTERNS OF THE LUNEBURG LENS
      IF(MO .EQ.0) GO TO 13
13      STOP
      END

      SUBROUTINE ETHETA(AK1, THI, ANGP1, ANGTI, STE, NUM, CJKRN,
1      RA, MOD, FRE, M1)
C      THIS SUBROUTINE WAS WRITTEN TO CALCULATE AND PLOT
C      THE THETA-COMPONENT OF THE ELECTRIC FIELD OF THE LUNE-
C      BERG LENS FOR ANY FEED FUNCTION OR ANY MEASURED FEED
C      DISTRIBUTION THAT CAN BE APPROXIMATED BY A CURVE
C      FITTING TECHNIQUE.
      IMPLICIT COMPLEX(C)
C      THE NEXT FOUR STATEMENTS CONTROL THE LABELING AND
C      TITLING OF THE GRAPHS PLOTTED BY SUBROUTINE DRAW.
      REAL LABEL '/'

```



```

REAL *8 TITLE(12)
READ(5,100) TITLE
100  FORMAT(6A8)
      COMPLEX CJ/(0.0,1.0)/
C     CFCT1 IS A FUNCTION DESCRIBING THE FAR FIELD OF THE
C     LUNEBERG LENS IN TERMS OF THE APPERTURE FIELD
C     DISTRIBUTION IN THE X-DIRECTION.
C     CFCT4 IS A FUNCTION DESCRIBING THE FAR FIELD OF THE
C     LUNEBERG LENS IN TERMS OF THE APPERTURE FIELD
C     DISTRIBUTION AS A FUNCTION OF THE
C     ANGULAR DISPLACEMENT FROM BEAM CENTER.
      EXTERNAL CFCT1,CFCT4
      DIMENSION THETA(400),CETHE(400),ETHEM(400),RADI(5),
1     FREQ(5)
      COMMON AK,ANGP,THETR,RAD,L3,L1
      COMMON/ALIM/ALIM1,ALIM2,THIC
      THIC=THI
      RAD=RA
      RADI(M1)=RA
      FREQ(M1)=FRE
      AK=AK1
      ANGP=ANGP1
      PIE=3.141592653589
      THET=ANGT1
      TH2=-THI/2.0
      TH3=THI/2.0
      ANORM=0.0
C     ENTER LOOP TO CALCULATE THE E-FIELD FOR NUM-POINTSIN
      DO 1 I=1,NUM
      L1=I
      L3=I
      THETR=THET*(PIE/180.0)
      CALL CWEDF(CFCT1,TH2,TH3,5,CETH1)
      L1=2
900   XL=ALIM1
      XU=ALIM2
      CALL CWEDF(CFCT4,XL,XU,375,CETH4)
      IF(L3.NE.-1) GO TO 1000
      L3=2
      GO TO 900
1000  CETH=CETH1*CETH4
      WRITE(6,96) CETH1,CETH4,CETH
96    FORMAT(' ',6E12.6)
C     WRITE(6,15)CETH
15    FORMAT(' ','CETH=',2F10.5)
      IF(ANORM.GE.CABS(CETH)) GO TO 2
      ANCRM=CABS(CETH)
      THETA(I)=THET
      CETHE(I)=CETH
      THET=THET+STE
      WRITE(6,95) THET,ANCRM
95    FORMAT(' ',2F12.5)
1     CCNTINUE
C     ENTER LOOP TO NORMALIZE AND CALCULATE THE MAGNITUDE
C     OF THE E-FIELD (EPHEM).
      DO 3 J=1,NUM
      CETHE(J)=CETHE(J)/ANORM
      ETHEM(J)=CABS(CETHE(J))
3     CCNTINUE
      WRITE(6,84)RADI(M1),FREQ(M1)
84    FORMAT('1','THETA-COMPONENT OF THE E-FIELD FOR LENS',
1     'RADIUS OF',F8.4,2X,'METERS AT',F8.4,2X,'GFZ',/' ',6X
2     'THETA',12X,'FIELD STRENGTH',10X,'COMPLEX FIELD ',
3     'STRENGTH')
      J=0
      DO 23 I=1,NUM
      WRITE(6,85)THETA(I),ETHEM(I),CETHE(I)
85    FORMAT(' ',F11.3,8X,F14.6,12X,F10.6,F10.6)
      J=J+1
      IF(J.LT.72)GO TO 23
      WRITE(6,84)RAD,FRE
      J=0

```



```

23  CCNTINUE
C   ENTER LOOP TO CALCULATE THE FIELD MAGNITUDES IN DECI-
C   BELS.
    DC 20 I=1,NUM
    ETHEM(I)=20.0*ALOG10(ETHEM(I))
20  CCNTINUE
    CALL DRAW(NUM,THETA,ETHEM,MOD,0,LABEL,TITLE,0,0,7,3,2,
90  12,6,8,1,LAST)
    RETURN
    END

```

```

SUBROUTINE CWEDF (CF,XL,XU,NX,CANS)

C   CWEDF WAS OBTAINED FROM LCDR. E.G.NEELY .
C   CWEDF IS A SUBROUTINE WHICH WILL NUMERICALLY
C   INTEGRATE A USER SUPPLIED FUNCTION BETWEEN SPECIFIED
C   LIMITS. (SINGLE PRECISION)
C   CF      - NAME OF FUNCTION SUBPROGRAM.  MUST BE
C   LISTED IN AN EXTERNAL STATEMENT.
C   XL      - LOWER LIMIT OF INTEGRATION
C   XU      - UPPER LIMIT OF INTEGRATION
C   NX      - APPROXIMATE NUMBER OF NCDES AT WHICH TO
C   EVALUATE THE FUNCTION.
C   CANS    - RESULT OF INTEGRATION
C

```

```

    IMPLICIT COMPLEX*8 (C)
    REAL*8 DXDX,XX
    REAL*4 CW(6)/82.,216.,27.,272.,27.,216./
    COMMON AK,ANGP,THETR,RAD,L3,L1
    IF(NX.LE.0) GO TO 900
    N=((NX+4)/6)*6+1
    DX=(XU-XL)/FLOAT(N-1)
    DXDX=DBLE(DX)
    NWIX=N/6
    X=XL
    CANS=-CF(X)*41.0
    IF(L3.EQ.-1) GO TO 1000
    IF(L1.EQ.1) GO TO 500
    IF(L3.NE.1) GO TO 500
    L3=2
500  DO 800 MX=1,NWIX
    DO 700 KX=1,6
    CANS=CANS+CW(KX)*CF(X)
    XX=DBLE(X)
    X=SNGL(XX+DXDX)
    700  CCNTINUE
    800  CONTINUE
    CANS=(CANS+41.0*CF(X))*DX/140.0
    RETURN
    900  WRITE(6,901) N
    901  FORMAT('OERROR IN CALLING PARAMETER ***** N = ',
1000  I5,' *****')
    RETURN
    END

```

```

C   COMPLEX FUNCTION CFCT1(X)
C   CFCT1 IS A FUNCTION WHICH DESCRIBES THE FAR-FIELD
C   VARIATIONS OF THE E-FIELD AS A FUNCTION OF THE LUNE-
C   BERG LENS HEIGHT.
    IMPLICIT COMPLEX(C)
    COMPLEX CJ/(0.0,1.0)/
    COMMON AK,ANGP,THETR,RAD,L3,L1
    COMMON/ALIM/ALIM1,ALIM2,THIC
    CEX=CJ*AK*SIN(THETR)*COS(ANGP)*X
    CFCT1=CEXP(CEX)*COS(X*3.14159/THIC)*(1.0+CCS(THETR))*
1  CCS(ANGP)
    RETURN
    END
C   COMPLEX FUNCTION CFCT4(ANG)
C   CFCT4 IS A FUNCTION WHICH DESCRIBES THE FAR FIELD
C   VARIATIONS OF THE E-FIELD AS A FUNCTION OF ANG
C   (THE ANGLE FROM BEAM CENTER). TO DO THIS LSQPL2 IS

```



```

C      UTILIZED TO FIT A CURVE TO THE MEASURED FEED FUNCTION
C      AND COMBINES THIS WITH THE OTHER ANGULAR VARIATIONS
C      OF THE FAR-FIELD EQUATIONS.
      IMPLICIT REAL*8(D)
      IMPLICIT COMPLEX(C)
      CCMPLX CJ/(0.0,1.0)/
      DIMENSION DTHETA(100),DMAG(100),DA(20),DWI(80),DY(80),
1      DELY(80),A(20),DSA(20),THETA(100),EMAG(100),DTHE(100)
      REAL*8 DTITL(10)/10*' '//
      COMMON AK,ANGP,THETR,RAD,L3,L1
      COMMON/ALIM/ALIM1,ALIM2,THIC
C      L3 WILL BE EQUAL TO 1 ON THE FIRST CALL OF CFCT4
C      AND WILL PROCEED THROUGH THE NEXT STEPS DOWN TO 600
C      IN ORDER TO CALCULATE THE POLYNOMIAL COEF. THAT
C      DESCRIBE THE FEED FUNCTION.
C      IF L3 IS NOT 1, THEN THE POLYNOMIAL COEF. HAVE BEEN
C      CALCULATED BY A PREVIOUS PASS.
      IF(L3.NE.1)GO TO 600
      READ(5,200)M,N
200    FORMAT(I3/I2)
      READ(5,400)(DTHETA(I),DMAG(I),I=1,N)
400    FORMAT(F10.7,F12.6)
      DO 60 J=1,N
60     DMAG(J)=DSQRT(DMAG(J))
      DO 50 I=1,N
50     DTHE(I)=DTHETA(I)*(3.1425926500/180.000)
      ALIM1=DTHE(1)
      ALIM2=DTHE(N)
      DO 5 I=1,N
5     DWI(I)=1.000
      CALL LSQLP2(N,M,DTHE,DMAG,DWI,DY,DELY,DA,CSA,DTITL)
      L=1-M
      DO 6 I=1,L
6     A(I)=DA(I)
      THETA(I)=DTHETA(I)
      WRITE(6,300)(I,A(I),I=1,L)
300    FORMAT(' ','A(',I4,')=' ',F18.6)
      L3=-1
      RETURN
600    EM=A(1)
      DO 4 J=2,L
4     ANGE=ANG**((J-1))
      IF(ABS(ANGE).LT.10.E-70) GO TO 7
      EM=EM+A(J)*ANGE
C      EA1 IS A FUNCTION WHICH DESCRIBES THE FEED VARIATIONS
C      OVER THE PLANE OF THE LENS.
7     EA1=EM
      CER=CJ*AK*RAD*(COS(ANG)*(COS(THETR)-1.0)-SIN(ANG)*
1     SIN(THETR)*SIN(ANGP))
C      THE SQRT(1.0/COS(ANG)) TERM IS THE ONLY PART OF THIS
C      EQUATION ASSOCIATED WITH THE LENS FUNCTION.
3     THE REMAINDER IS FROM THE APPLICATION OF THE APERTURE
C      FIELD METHOD TO THE SEMI-CIRCULAR APERTURE. TO MOD-
C      IFY THIS PROGRAM TO PREDICT THE CONSTANT-K LENS FAR
C      FIELD PATTERNS CHANGE THIS FUNCTION. THE CORRECT PHASE
C      TERMS ARE ALREADY INCLUDED.
      CFCT4=CEXP(CER)*EA1*SQRT(COS(ANG))
      RETURN
      END

```



## BIBLIOGRAPHY

1. Luneberg, R.K., The Mathematical Theory of Optics, Brown University Press, 1944.
2. Bryant, M.B. and Hunt B.R., "Luneberg Lens Antenna Testing for ECM Application," Naval Electronics Laboratory Center, 1 April 1969.
3. Born and Wolf, Principles of Optics, Pergamon Press, 1970.
4. Peeler, G.M.D., and Archer, D.H., "A Two Dimensional Microwave Luneberg Lens," IRE Transactions on Antennas and Propagation, July 1953, pp.
5. Walters, C.H., Traveling Wave Antennas, McGraw-Hill, 1965.



# INITIAL DISTRIBUTION LIST

|   | No. Copies |
|---|------------|
| 1. Defense Documentation Center<br>Cameron Station<br>Alexandria, Virginia 22314  | 2          |
| 2. Library, Code 0212<br>Naval Postgraduate School<br>Monterey, California 93940  | 2          |
| 3. Dr. Richard W. Adler (thesis advisor)<br>Department of Electrical Engineering - code 52Ab<br>Naval Postgraduate School<br>Monterey, California 93940 | 1          |
| 4. LT Robert B. Birchfield<br>613 South Perry Street<br>Attica, Indiana 47918   | 1          |
| 5. Dr. R.C. Hansen<br>17100 Ventura Blvd.<br>Encino, California 91316   | 1          |
| 6. Director, Naval Research Center<br>Washington D.C. 20375<br>ATTN: Charles T. Bender  | 1          |
| 7. Commanding Officer<br>Naval Electronic Laboratory Center<br>271 Catalina Blvd.<br>San Diego, California 92152<br>ATTN: M.B. Bryant                   | 1          |



| REPORT DOCUMENTATION PAGE  |                       | READ INSTRUCTIONS<br>BEFORE COMPLETING FORM                              |
|--|-----------------------|--|
| 1. REPORT NUMBER   | 2. GOVT ACCESSION NO. | 3. RECIPIENT'S CATALOG NUMBER  |
| 4. TITLE (and Subtitle)<br><br>The Far Field Analysis of Parallel Plate<br>Luneberg Lenses for Various Feeds   |                       | 5. TYPE OF REPORT & PERIOD COVERED<br>Master's Thesis;<br>September 1973 |
|  |                       | 6. PERFORMING ORG. REPORT NUMBER   |
| 7. AUTHOR(s)<br><br>Robert Boyd Birchfield   |                       | 8. CONTRACT OR GRANT NUMBER(s)   |
| 9. PERFORMING ORGANIZATION NAME AND ADDRESS<br><br>Naval Postgraduate School<br>Monterey, California 93940   |                       | 10. PROGRAM ELEMENT, PROJECT, TASK<br>AREA & WORK UNIT NUMBERS           |
| 11. CONTROLLING OFFICE NAME AND ADDRESS<br><br>Naval Postgraduate School<br>Monterey, California 93940   |                       | 12. REPORT DATE<br>September 1973  |
|  |                       | 13. NUMBER OF PAGES  |
| 14. MONITORING AGENCY NAME & ADDRESS (if different from Controlling Office)<br><br>Naval Postgraduate School<br>Monterey, California 93940   |                       | 15. SECURITY CLASS. (of this report)<br><br>Unclassified                 |
|  |                       | 15a. DECLASSIFICATION/DOWNGRADING<br>SCHEDULE                            |
| 16. DISTRIBUTION STATEMENT (of this Report)<br><br>Approved for public release; distribution unlimited.  |                       |  |
| 17. DISTRIBUTION STATEMENT (of the abstract entered in Block 20, if different from Report)   |                       |  |
| 18. SUPPLEMENTARY NOTES  |                       |  |
| 19. KEY WORDS (Continue on reverse side if necessary and identify by block number)<br><br>Luneberg Lens<br>Aperature Field<br>Far Field Radiation<br><br>Microwave Antenna   |                       |  |
| 20. ABSTRACT (Continue on reverse side if necessary and identify by block number)<br><br>This thesis developed expressions for the aperature fields and inte-<br>gral equations for the far field radiation characteristics of the Parallel<br>Plate Luneberg Lens Microwave Antenna operating in the TEM or TE <sub>10</sub> modes.<br>These expressions were programmed on a difital computer to predict the<br>far field radiation patterns for several feed systems. Experimentation<br>produced far field radiation patterns that were very close to the theor-<br>etical patterns for the TE <sub>10</sub> mode lens and substantially different for<br>the TEM mode lens. |                       |  |







Thesis

146097

B5434 Birchfield

c.1

The far field analysis  
of parallel plate Lune-  
berg Lenses for various  
feeds.

Thesis

146097

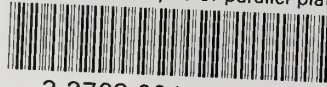
B5434 Birchfield

c.1

The far field analysis  
of parallel plate Lune-  
berg Lenses for various  
feeds.

thesB5434

The far field analysis of parallel plate



3 2768 001 03656 9

DUDLEY KNOX LIBRARY